PERGAMON

Deep-Sea Research I 49 (2002) 211–243

DEEP-SEA RESEARCH
PART I

www.elsevier.com/locate/dsr

On the Atlantic inflow to the Caribbean Sea

William E. Johns[a,*], Tamara L. Townsend[b], David M. Fratantoni[c], W. Douglas Wilson[d]

[a] *Rosenstiel School of Marine and Atmospheric Science, University of Miami, 4600 Rickenbacker Causeway, Miami, FL 33149, USA*
[b] *Naval Research Laboratory, Stennis Space Center, MS 39529, USA*
[c] *Department of Physical Oceanography, Woods Hole Oceanographic Institution, Woods Hole, MA 02543, USA*
[d] *Physical Oceanography Division, NOAA/AOML, 4301 Rickenbacker Causeway, Miami, FL 33149, USA*

Received 26 September 2000; received in revised form 4 June 2001; accepted 4 June 2001

Abstract

New observations are summarized that lead to the first comprehensive description of the mean inflow distribution in the passages connecting the Atlantic Ocean with the Caribbean Sea. The total Caribbean inflow of 28 Sv is shown to be partitioned approximately equally between the Windward Islands Passages (~10 Sv), Leeward Islands Passages (~8 Sv), and the Greater Antilles Passages (~10 Sv). These results are compared to a numerical model study using a 6-layer, 1/4° resolution Atlantic Basin version of the NRL Layered Ocean Model. Results from two simulations are described, including a purely wind-forced model driven by Hellerman and Rosenstein (J. Phys. Oceanogr. 13 (1983) 1093) monthly winds, and a model with an additional 14 Sv meridional overturning cell driven by inflow/outflow ports at the northern (65°N) and southern (20°S) model boundaries. The purely wind-driven version of the model exhibits a total Caribbean inflow of 17 Sv, consistent with expectations from steady, non-topographic Sverdrup theory. Nearly all of the wind-driven inflow occurs north of Martinique at latitude ~15°N. The net transport through the Lesser Antilles passages south of 15°N (Grenada, St. Vincent, and St. Lucia passages) is nearly zero when the model is forced by winds alone. The addition of a 14 Sv meridional cell in the model increases the net Caribbean inflow to 28 Sv, with nearly all of the additional 11 Sv of inflow entering through the southern Lesser Antilles passages. The modeled inflow distribution resulting from the combined wind and overturning forced experiment is found to compare favorably with the observations.

The seasonal cycle of the total inflow in the combined forcing experiment has a mixed annual/semiannual character with maximum in spring and summer and minimum in fall, with a total range of about 4 Sv. The seasonal cycle of the Florida Current resulting from this inflow variation is in good qualitative agreement with observations. Most of the seasonal inflow variation occurs through the Windward Islands passages in the far southern Caribbean, whose annual cycle slightly leads that of the Florida and Yucatan Currents. Variability of the modeled inflow on shorter time scales shows a dramatic change in character moving northward along the Antilles arc. The southern passages exhibit large fluctuations on 30–80 day time scales, which decay to very small amplitudes north of Dominica. Much of this variability is caused by North Brazil Current Rings that propagate northwestward from the equatorial Atlantic and interact with the abrupt island arc topography. The total range of transport variability in individual passages predicted by the model is consistent with observations. However, observations are presently too limited to confirm the seasonal cycles or variability spectra in the Caribbean passages.

Keywords: Caribbean Sea; Circulation; Transports

*Corresponding author.
E-mail address: wjohns@rsmas.miami.edu (W.E. Johns).

0967-0637/02/$ - see front matter
PII: S0967-0637(01)00041-3

1. Introduction

The western boundary of the North Atlantic subtropical gyre is composed of a complex island chain, the Antilles Island arc, extending southward from the Bahamas to the northern coast of South America. Mass conservation requires that the inflow from the Atlantic through the passages in this chain combine to feed a mean Florida Current transport of approximately 30 Sv, with a superimposed annual cycle of ± 3 Sv (Niiler and Richardson, 1973; Schott et al., 1988). Certain of the Antilles passages have been intensively studied in the past, including the southernmost passages through the Lesser Antilles (Stalcup and Metcalf, 1972) and the northern Bahamian passages (Leaman et al., 1995; Atkinson et al., 1995). However, until recently many of the other passages had been poorly sampled, and consequently little was known about the overall distribution of the mean Atlantic inflow to the Caribbean. Recent observational efforts (Wilson and Johns, 1997; Johns et al., 1999) have provided a much improved picture of the average inflow distribution through the eastern Caribbean passages, but little is still known about the seasonal variation of the inflow or the amplitudes and time scales of the variability.

Ideas on the forcing mechanisms that drive the Caribbean inflow and Florida Current transport have evolved considerably in recent years. Previously viewed as simply a return current for the wind-driven Sverdrup flow of the subtropical gyre (Leetmaa et al., 1977), the Florida Current is now known to be an important conduit for northward transport of upper ocean waters in the global thermohaline circulation (Schmitz and Richardson, 1991). The Atlantic branch of this cell, referred to here as the Meridional Overturning Cell (MOC), transports approximately 15 Sv of cold deep water southward across the equator, balanced by a northward return flow of upper ocean South Atlantic waters. This return flow originates partly from intermediate waters passing through Drake Passage from the Pacific Ocean, and partly from upper thermocline waters of the Indian Ocean that leak around South Africa from the Agulhas Current and its retroflection (Gordon, 1986; Rintoul, 1991; Gordon et al., 1992; Schmitz, 1996). These waters join together in the southeastern Atlantic and are transported equatorward in the Benguela Current (Garzoli and Gordon, 1996). The exact pathways of this MOC return flow through the tropical Atlantic are poorly understood at present, although it is known that substantial upwelling and modification of these waters occurs in the equatorial region (Roemmich, 1983). Measurements in the western tropical Atlantic (Schott et al., 1993; Johns et al., 1998) suggest that the North Brazil Current is the main pathway for transport of these modified South Atlantic waters northward from the equator. Their entry into the subtropical gyre appears to involve direct pathways along the tropical western boundary as well as through the ocean interior (Schmitz and McCartney, 1993; Mayer and Weisberg, 1993; Fratantoni et al., 2000). Large anticyclonic eddies that pinch off from the North Brazil Current also contribute to this intergyre exchange and may account for a significant fraction of the total MOC return flow in the Atlantic (Johns et al., 1990; Richardson et al., 1994; Didden and Schott, 1993; Fratantoni et al., 1995; Goni and Johns, 2001). Ultimately these modified South Atlantic waters are carried northward and westward into the southern limb of the subtropical gyre and transported northward along the western boundary in the Gulf Stream system (Schmitz and Richardson, 1991; Schmitz and McCartney, 1993).

The purpose of this paper is to examine, through the use of the Naval Research Laboratory (NRL) Atlantic basin model, how the wind-driven and MOC circulations might be expected to combine to produce the total inflow to the Caribbean. The focus is two-fold. First, we show how the circulation patterns and transports through the Caribbean passages change when a realistic MOC is added to a purely wind-driven model. The main conclusion is that the southernmost channels passing into the Caribbean are the dominant entry point for the MOC flow to the Caribbean, and that the distribution of transport through the Caribbean passages predicted by the combined wind/MOC model is reasonably consistent with available observations. Second, we show how the seasonal transport cycles of the various passages combine to produce the seasonal cycle of the

Yucatan and Florida Currents, and compare the results to Sverdrup predictions and other numerical model results. Again, the southern passages of the Caribbean are shown to play a dominant role in the seasonal cycle. Finally, we describe the mesoscale variability of the passage transports and show that this variability is considerably more energetic in the model that includes a realistic MOC.

Before proceeding to the model results, we provide a summary of available observations on the inflow to the Caribbean Sea. This summary includes recent observations in the eastern Caribbean passages and in the Greater Antilles passages, including some previously unpublished data.

2. The observed inflow to the Caribbean Sea

The mean transport of the Florida Current is now well established at a value of 31.5 ± 1.5 Sv (Lee et al., 1996). Most of the Atlantic inflow feeding the Florida Current enters the Caribbean between Cuba and South America, since the transport through Yucatan Channel is comparable to that of the Florida Current. There are nine passages along the Antilles arc between Cuba and South America with sill depths greater than about 400 m through which significant transport contributions could occur (Fig. 1). Geographically these can be grouped into a set of seven main passages south of 19°N through the Lesser Antilles arc, which runs almost north–south along 61–63°W, and two major passages (the Mona and Windward Passages) between 18 and 20°N along the westward tending Greater Antilles arc. It is convenient to further subdivide the Lesser Antilles passages into a set of "Windward Island" passages south of 15°N (Grenada, St. Vincent, and St. Lucia passages), and "Leeward Island" passages between 15 and 19°N (Dominica, Guadeloupe, Antigua, and Anegada passages). It is common in the literature for the total

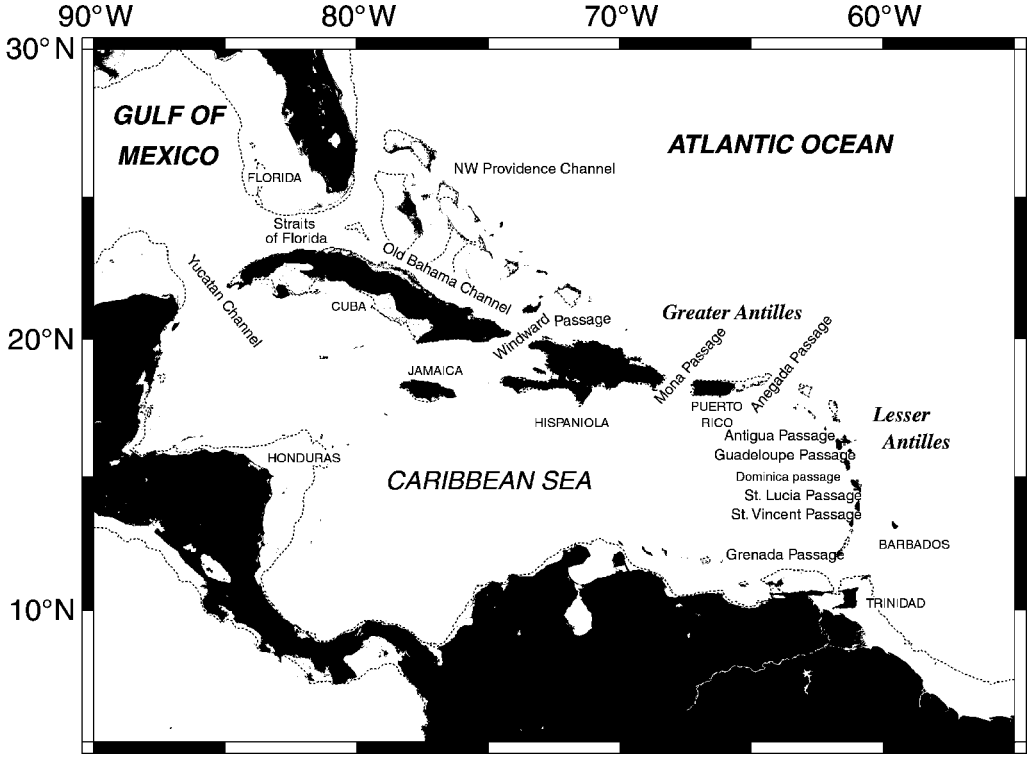

Fig. 1. The Caribbean Sea. The main passages between the Atlantic Ocean and Caribbean Sea are labeled.

inflow between South America and the Virgin Islands (along approximately 65°W) to be referred to as the "eastern Caribbean" inflow, which, in accordance with the above definitions, is the same as the inflow through the Lesser Antilles passages.

Model (1950) was the first to provide a description of the inflow through all of the Caribbean passages, based on the observations of Pillsbury (1891). He found a total inflow to the Caribbean of 28 Sv (1 Sv = 10^6 m^3 s^{-1}), of which 24 Sv flowed through the Lesser Antilles passages. Of the 24 Sv entering the Lesser Antilles, approximately three-fourths (18 Sv) was found to flow through the Leeward Island passages, with only 6 Sv entering through the Windward Island passages in the south. Certain features of this inflow distribution are questionable and based on very limited data; for example, Model found negligible inflow through both the Grenada and Windward Passages, which have more recently been identified as major inflow channels.

Geostrophic transport estimates by Gordon (1967) suggested a total inflow through the eastern Caribbean of 26–33 Sv, with less than 5 Sv of inflow through Windward Passage. Worthington (1976) assigned a relatively greater importance to Windward Passage (10 Sv) and a smaller total inflow (20 Sv) through the eastern Caribbean. Roemmich (1983) found a total transport of approximately 22 Sv through the eastern Caribbean and 7 Sv through Windward Passage based on an inverse calculation. However, none of the above studies were able to determine the detailed structure or distribution of the inflow through the Lesser Antilles.

Individual passages in the eastern Caribbean have been sampled at various times by Metcalf (1976), (Anegada Passage); Stalcup and Metcalf (1972), (Grenada, St. Vincent, St. Lucia, and Dominica Passages); and Brooks (1978), (St. Lucia Passage). Most of these studies were of relatively short duration and found significant tidal and synoptic variability in the passage transports. Of particular note was Stalcup and Metcalf's (1972) finding of a transport of 25 Sv through the Windward Island passages from repeated measurements over a 5-week period in March–April 1970, which suggested that the net inflow through the eastern Caribbean was strongly concentrated in the southern Lesser Antilles. Schmitz and Richardson (1991) reanalyzed the Stalcup and Metcalf data and concluded that 22 Sv of the Florida Current transport could be accounted for by inflow through these southern passages, with most of the remainder (7 Sv) entering through Windward Passage in the north.

In recent years there has been a large increase in the available data base for the eastern Caribbean passages, which in part has motivated the present study. Most importantly, in many passages there are now enough repeat measurements that meaningful estimates can be made of the average passage transports and their ranges of variability. The most definitive measurements are from Wilson and Johns (1997), updated with the more recent data shown in Table 1. Measurements in the Leeward Islands passages (Johns et al., 1999; Table 1) have also provided new baseline estimates for many of the historically poorly sampled passages in the Lesser Antilles chain.

Table 2 summarizes the above observations together with other historical estimates of the transports through main passages to the Caribbean Sea. The estimates shown in Table 2 come from a variety of different sources using different methods, and some may be more accurate than others. Those transport values that are derived from repeated direct velocity measurements, such as in Table 1, and that include estimates of statistical uncertainty, are relied upon most heavily in the following synopsis.

2.1. The Windward Islands Passages

The passages between the Windward Islands (composed of Grenada, St. Vincent, and St. Lucia Passages) are probably the best studied of all the Antilles passages (Stalcup and Metcalf, 1972; Wilson and Johns, 1997). The combined transport through these passages as measured by Wilson and Johns (1997; hereafter WJ97), updated in Table 1, is 10.1 ± 2.4 Sv. Grenada Passage accounts for slightly more than half of this total inflow (5.7 ± 0.8 Sv), followed in importance by St. Vincent (2.9 ± 0.8 Sv) and St. Lucia (1.5 ± 0.8 Sv) passages. These estimates come from a total of 10–12

Table 1
Transport estimates derived from shipboard occupations of the Caribbean Passages, after Wilson and Johns (1997), updated with results from 5 additional cruises. Not all passages were sampled on each cruise. Average transports and related statistics from all available estimates for each passage are shown at the bottom. The quantity labeled "Mean" is the average transport from only those cruises with full water column directly velocity measurements (cruises 5 and later) the quantity labeled "Mean (all)" is the average of all cruises including early ones where part of the deep flow in the passages was determined geostrophically. The former is used for the final transport values in the paper, and the standard errors listed for each passage are also based on this data

		Passage							
Cruise		Grenada	St. Vincent	St. Lucia	Dominica	Guadeloupe	Antigua	Anegada	Mona
1	Dec 91	6.9	5.9	0.1					
2	May 92	0.1	2.0	0.5					
3	Sep 92		4.9	1.4	0.5				
4	Dec 92	2.6	2.2	2.2					
5	Jun 93	10.6	5.3	1.2					
6	Apr 94	2.6	−0.6						
7	Jul 94	5.8	5.2	2.0	−0.1	1.9	0.6	3.3	
8	Dec 94			−0.2					
9	Sep 95	5.4	2.8	3.2					
10	Mar 96	4.0	−0.1	0.8	1.8	1.1	4.4	3.5	3.4
11	Jul 96	5.6	3.4	3.4	1.1	0.6	3.3	2.2	1.7
12	Jun 97	4.6	3.7	4.6	2.5	−0.3	3.4	2.0	
13	Oct 98	6.7	3.2	−3.0	2.8	2.4	4.0	0.1	
Mean		5.7±2.4	2.9±2.2	1.5±2.4	1.6±1.2	1.1±1.1	3.1±1.5	2.5±1.4	2.6±1.2
Mean (all)		5.0±2.8	3.2±2.1	1.4±2.0	1.4±1.1	1.1±1.1	3.1±1.5	2.5±1.4	2.6±1.2
Std. error		0.8	0.8	0.8	0.5	0.5	0.7	0.6	1.2
		Windward Islands 10.1±2.4			Leeward Islands 8.3±2.3				
		Lesser Antilles 18.4±4.7							

independent measurements of transport in these passages carried out in different seasons over a 7-year period. The results in Table 1 include transport measurements from an additional five cruises subsequent to those described in WJ97. These additional transports were obtained by the same methods used in WJ97, and the reader is referred to that paper for details on the measurement techniques and transport estimation methods. The relatively small error bars on the mean transports shown in Table 1 are attributable to the large number of independent samples rather than small variability in the passage transports, which typically have a range of about twice their mean value. For example, the Grenada Passage transport has a total range of 10.5 Sv (Table 1), from a minimum of nearly zero (0.1 Sv) to a maximum of 10.6 Sv.

The earlier measurements of Stalcup and Metcalf (1972) suggest a much larger transport through the Windward Islands passages; however, it should be noted that their measurements were collected during a single 2-month observation period in 1970, and their results differed significantly between two independent measurement techniques (see Table 2). The smaller of their estimates (15.3 Sv) is within the range of observed transports shown by WJ97 (and Table 1), and is in reasonable agreement with the mean value obtained from Table 1 of 10.1±2.4, considering the short period of the Stalcup and Metcalf measurements.

For a detailed review of the observations and flow structures observed in the Windward Islands Passages, the reader is referred to Wilson and Johns (1997).

Table 2
Comparison of modeled versus observed passage transports

Passage	Model B	Observation	Source
	Mean (Std. Dev.)	Mean (Std. Dev., Std. err)	
Grenada	5.0 (2.1)	4.4–9.6[a]	Stalcup and Metcalf (1972)
		5.7 (2.4, 0.8)	(This study; Table 1)
St. Vincent	5.2 (1.3)	7.9–9.7[a]	Stalcup and Metcalf (1972)
		2.9 (2.2, 0.8)	(This study; Table 1)
St. Lucia	2.1 (0.5)	3.0–5.9[a]	Stalcup and Metcalf (1972)
		1.7 (3.0)	Brooks (1978)
		1.5 (2.4, 0.8)	(This study; Table 1)
Windward Islands (Grenada St. Vincent, and St. Lucia)	12.3 (2.4)	15.3–25.2[a]	Stalcup and Metcalf (1972)
		13.0 (2.0)	Mazeika et al. (1980)
			Febres-Ortega and Herrera (1976); ("Tobago-Barbados" section)
		10.1 (4.0, 2.4)	(This study; Table 1)
Dominica	1.9 (0.7)	2.6	Stalcup and Metcalf (1972)
		1.6 (1.2, 0.5)	(This study; Table 1)
Guadeloupe	1.6 (0.3)	1.1 (1.1, 0.5)	(This study; Table 1)
Antigua	2.1 (0.4)	3.1 (1.5, 0.7)	(This study; Table 1)
Anegada	3.8 (0.8)	2.0–2.5	Metcalf (1976)
		2.5 (1.4, 0.6)	(This study; Table 1)
		2.4 (2.8, 0.9)	<200 m, Johns et al. (1999)
Leeward Islands (Dominica, Guadeloupe, Antigua, and Anegada)	9.4 (1.2)	8.3 (2.6, 2.3)	(This study; Table 1)
Mona	2.5 (0.5)	0.5[b]	Roemmich (1981)
		2.6 (1.2, 1.2)	(This study; Table 1)
		2.8 (2.1, 0.9)	<200 m, Johns et al. (1999)
Windward	4.3 (2.0)	7.0	Roemmich (1981)
		9.0	Nelepo et al. (1976)
		6.0–7.0	Wunsch and Grant (1982)
		2.2 (1.5, 0.5)	<200 m, Johns et al. (1999) ("Great Inagua Passage")
Greater Antilles (Mona and Windward)	6.8 (2.1)	~10.0 (4.0?)	This study + Roemmich (1981)
Old Bahama	1.5 (0.7)	1.9 (1.7)	Atkinson et al. (1995)
NW Providence	2.5 (0.9)	2.0	Richardson and Finlen (1967)
		1.2 (2.0)	Leaman et al. (1995)

[a] Stalcup and Metcalf (1972) used both lowered current meters and free-falling transport profilers (dropsondes). The transport values determined from the lowered current meter technique were larger by up to a factor of two and may be overestimates.

[b] Roemmich's original estimate of the geostrophic transport through Mona Passage was 4.0 Sv, before application of inverse model constraints.

2.2. The Leeward Islands Passages

The Passages through the Leeward Islands (Dominica, Guadeloupe, Antigua, and Anegada Passages) are less well sampled than the Windward Islands passages, and only recently have detailed measurements been made in some of them (Table 1). Previously, there were no published estimates of transport through the Guadeloupe or Antigua Passages, apart from those of Model (1950), and considerable uncertainty existed as to the mean transports through the Anegada and Dominica Passages (Metcalf, 1976; Stalcup and Metcalf, 1972; WJ97). The Anegada Passage is distinguished from the rest of the Lesser Antilles passages by a much greater sill depth of 1900 m, which permits exchange between the Caribbean and Atlantic at levels below the direct influence of the subtropical gyre circulation. Anegada Passage is the sole pathway for ventilation of the abyssal Venezuelan and Colombian basins of the southern Caribbean from the Atlantic. The inflow of North Atlantic Deep Water through this passage and its subsequent spillage into the deep Caribbean has been studied by many investigators (Worthington, 1955; Stalcup et al., 1975; Sturges, 1975; Fratantoni et al., 1997; MacCready et al., 1999). The transport associated with this overflow process is small however, approximately 0.2 Sv, and is negligible in the total transport budget for the Caribbean.

The estimated mean transports through the Leeward Islands passages, from the new data in Table 1, are 1.6 ± 0.5, 1.1 ± 0.5, 3.1 ± 0.7, and 2.5 ± 0.6 Sv, for Dominica, Guadeloupe, Antigua, and Anegada Passage, respectively. The total inflow through the Leeward Islands is therefore estimated at 8.3 ± 2.3 Sv. This inflow is comparable to that through the Windward Islands passages, but it is concentrated more in the northern part of the Leeward Island chain, with the Antigua and Anegada Passages being the dominant inflow channels.

The observations of transport through the Anegada Passage listed in Table 2 include geostrophic estimates from hydrographic surveys in the 1970s as well as the more recent direct current measurements. Metcalf (1976) estimated the total inflow through Anegada passage to be approximately 1.4 Sv from geostrophic current measurements collected in March–April 1972. Considering only the upper 700 m they found a somewhat larger inflow of 2.0–2.5 Sv. The estimate of 2.5 Sv for Anegada Passage from Table 1 is consistent with Metcalf's estimate for the upper 700 m inflow, and also with the Johns et al. (1999) estimate of 2.4 ± 0.9 Sv inflow from 9 repeat shipboard ADCP transects across the passage. The latter transport estimate includes only the contribution within the upper 200 m of the water column, which suggests that the total inflow could be larger than the 2.5 Sv derived from the smaller set of full-depth occupations contained in Table 1. Measurements in Dominica Passage by Stalcup and Metcalf (1972), as re-analyzed by Schmitz and Richardson (1991, hereafter SR91), suggested an inflow through Dominica passage of 2.6 Sv, which is outside the error bounds of the mean transport estimate of 1.6 ± 0.5 Sv from Table 1, but within the maximum transport of 2.8 Sv observed in the 8 occupations of the passage listed in Table 1. The transport estimates for Guadeloupe, Antigua, and Anegada passages shown in Table 1 are based on fewer occupations (5–6) than in Dominica or the Windward Islands Passages, but nevertheless appear to be converging on stable mean transport values.

2.3. The Greater Antilles Passages

The two passages through the Greater Antilles, Mona and Windward, are very different from one another in terms of their sill depths. Mona Passage, with a sill depth of $\sim$400 m, is the shallowest major passage in all of the Antilles; Windward Passage, with a sill depth of $\sim$1700 m, is deeper than all but Anegada Passage. The deep inflow through the Windward Passage is less well studied than that in the Anegada Passage but may play a similar role in replenishing abyssal waters of the Cayman and Yucatan basins in the northern Caribbean. Again the mean inflow associated with this process is small and does not significantly impact the transport balance of the upper ocean that is the focus of this paper.

The only study that provides a suitably large ensemble of repeated direct measurements in the

Greater Antilles passages is the study by Johns et al. (1999) using shipboard acoustic Doppler profiler data, which however is limited to the upper 200 m of the water column. Their estimate of the upper 200 m transport through Mona Passage is 2.8 ± 0.9 Sv. Two full-depth occupations of Mona Passage are included in Table 1, and these show total inflow transports of 3.4 and 1.7 Sv for an average of 2.6 Sv. Roemmich's (1981) indirect estimate from an inverse model suggests a lower inflow transport of 0.5 Sv. However, it should be noted that Roemmich's transport estimate was strongly affected by his inverse model constraints, as the geostrophic transport through Mona Passage relative to the bottom calculated by Roemmich prior to adjustment by the inverse calculation was 4.0 Sv. Thus, Mona Passage appears to be a significant inflow channel with a mean transport of approximately 3 Sv.

The transport through Windward Passage has been estimated at 9.0 Sv by Nelepo et al. (1976) and 7.0 Sv by Roemmich (1981), using geostrophic estimates from hydrographic data. (Roemmich's inverse model estimate of 7.0 Sv in this case closely agrees with his initial transport calculation.) Wunsch and Grant (1982) also found a value of 6–7 Sv from their North Atlantic inverse model. Johns et al. (1999) obtained a mean inflow of 2.2 ± 1.5 Sv in the upper 200 m from 9 repeat occupations of the "Great Inagua" Passage, which lies just east of Windward Passage between the coast of Hispaniola and Great Inagua Island. This channel presumably carries most of the inflow that enters Windward Passage plus a small contribution that may bypass Windward Passage to flow westward into the Old Bahama Channel. The upper 200 m inflow of 2.2 Sv suggests a somewhat smaller total inflow through the Windward Passage than the available estimates of 7–9 Sv, since a transport of that size would require a nearly uniform inflow down to the base of the main thermocline ($\sim$800 m) of strength equal to that in the upper 200 m. A subset of these sections which included full-depth geostrophic and absolute velocity measurements yielded a mean transport estimate of 5.2 Sv through Great Inagua Passage (E. Johns, pers. comm.). A single occupation of Windward Passage with direct current measurements in 1998 (D. Wilson, pers. comm.) found less than 1 Sv of inflow in the upper 1000 m, which is, however, unlikely to be representative of average flow conditions. From the available observations a mean transport through Windward Passage anywhere in the range of 3–9 Sv seems possible. Further direct measurements are clearly needed to resolve the mean inflow and variability in this passage.

Since the mean transports through the Greater Antilles passages, especially Windward Passage, are poorly constrained by direct observations, it is useful to compare the above results with an indirect estimate of their net transport formed by differencing the better known transports through Yucatan Channel and the Lesser Antilles. The Yucatan Channel transport is approximately 28 Sv, as given by the difference between the Florida Current transport at 27°N (31.5 Sv) and the sum of the Old Bahama Channel and Northwest Providence channel inflows ($\sim$3 Sv; Table 2). The total transport through the Lesser Antilles, from the data in Table 1, is 18.4 Sv, which therefore requires a mean inflow of approximately 10 Sv through the Greater Antilles passages. If the Mona Passage accounts for 3 Sv of this inflow, then this leaves 7 Sv for Windward Passage, which is in good agreement with the Roemmich (1981) and Wunsch and Grant (1982) inverse model estimates. Therefore we conclude that a total inflow of approximately 10 Sv occurs through the Greater Antilles passages with about two-thirds of this flowing through Windward Passage and one-third through Mona Passage.

In summary, the observations suggest a nearly equal partitioning of the Caribbean inflow between the Windward Islands Passages ($\sim$10 Sv), the Leeward Islands Passages ($\sim$8 Sv), and the Greater Antilles Passages ($\sim$10 Sv). Later these observed transports will be compared with the numerical model predictions.

3. The model simulations

The numerical model used in this study is the Naval Research Laboratory (NRL) hydrodynamic, nonlinear, primitive equation layered ocean

circulation model (NLOM). It was developed by Hurlburt and Thompson (1980) for use in the Gulf of Mexico and has since been expanded to include regional, basin, and global-scale configurations (Wallcraft, 1991) and additional features, including thermodynamics (Metzger and Hurlburt, 1996; Shriver and Hurlburt, 1997; Wallcraft and Moore, 1997). The Atlantic Basin version of the model is used in this study. The model domain, with realistic coastlines and topography, extends from 20°S to 65°N, with a horizontal grid resolution of 1/4° (Fig. 2). Model parameters are listed in Table 3. Six constant-density layers are used in the vertical, five of which are contained within the upper 1000 m (Table 4).

The model simulations are begun from rest, and are initialized with uniform layer thicknesses over the basin. The density in each layer is the basin-wide average from Levitus (1982). In the real ocean, all of these density layers outcrop in the subpolar North Atlantic. In the model, the upper layers should, therefore, go to zero thickness in this region. In NLOM, the layers are instead required to maintain a prescribed minimum

Table 3
Model parameters

Parameter	Value
Coefficient of horizontal eddy viscosity	300 m^2 s^{-1}
Latitude, longitude grid resolution	1/4°, 45/128° (27 km at 45°N)
Bottom drag coefficient	0.002
Coefficient of interfacial stress (excluding entrainment)	0
Coefficient of interfacial stress due to entrainment	1
Acceleration due to gravity	9.8 m s^{-2}
Thickness of layer k at which entrainment starts	50 m ($k = 1$) 40 m ($k = 2$–6)
Reference diapycnical mixing velocity	0.01 cm s^{-1}

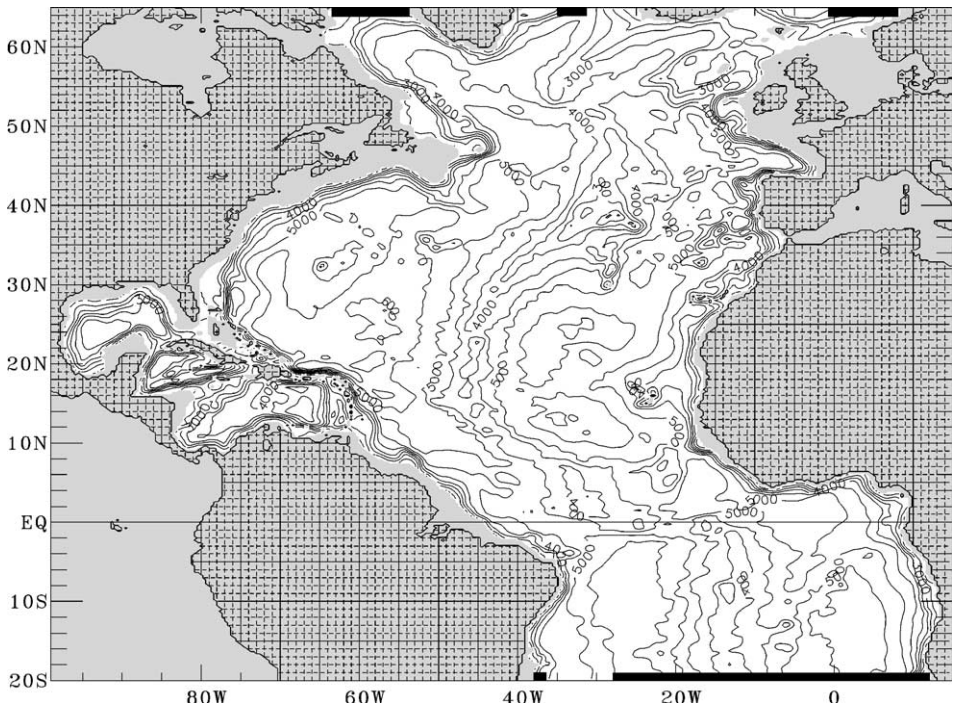

Fig. 2. The model domain and topography. The locations of the inflow and outflow ports used to drive the MOC in model B are indicated by black strips along the northern and southern boundaries. (See Table 4 for port transports in each layer.)

Table 4
Model layer densities, rest thicknesses, and port transports in the MOC-forced experiment. Positive transports are northward. See Fig. 2 for the locations of the inflow/outflow ports

Layer	Density (sigma-t)	Rest thickness (m)	Port transports (in Sverdrups)					
			20°S		65°N[a]			
			West	East	West	Central	East	Gibraltar
1	24.86	60	—	—	−0.5	—	−2.0	−0.5
2	26.03	115	—	7.0	−0.5	—	−2.0	−0.5
3	26.75	200	5.0	—	−0.4	—	−1.6	1.0
4	27.07	275	2.0	—	−0.3	—	−1.2	—
5	27.36	350	—	—	−0.3	—	−1.2	—
6	27.77	5500[b]	−14.0	—	4.0	6.0	—	—

[b] Minus amplitude of bottom topography above reference depth of 6500 m.
[a] Ports across 65°N correspond to: Davis Strait (“west”), Denmark Strait (“central”), and the Norwegian Current (“east”).

thickness in order to retain computational efficiency. For the uppermost layer a minimum thickness of 50 m is prescribed, which represents a nominal mixed layer depth. A slightly smaller value (40 m) is used for the remaining layers. When a layer thins to its minimum allowed thickness, water is entrained locally from the layer below in order to prevent the layer from thinning further. In the model this happens mostly in regions where wind-driven Ekman transports cause a divergence in the top layer, resulting in suction on the layers below. This process of “hydromixing” (Wallcraft, 1991) transfers mass and momentum to the entraining layer, but not density (which remains constant within each layer in this version of the model). To conserve mass within both the entraining layer and the layer below it, which loses mass during the entrainment process, there is a compensating global exchange of water from the upper layer to the layer below. This capability allows closed mean vertical circulations across layer interfaces within the model domain. It, therefore, also plays a role in the mechanism (described below) by which the Atlantic MOC is included in the model.

The dominant pattern of vertical mass exchange in the models is one of wind-driven upwelling from the thermocline to surface layers in the equatorial region and downwelling in the subtropics. A detailed study of these processes and associated diapycnal transports in a similar NRL Atlantic basin model simulation is given by Fratantoni (1996) and Fratantoni et al. (2000). Other recent applications of this model include an investigation of North Brazil Current ring formation and decay in the western tropical Atlantic (Fratantoni et al., 1995), and a study of the propagation of eddy features through the Caribbean and their influence on Loop Current variability in the Gulf of Mexico (Murphy et al., 1999).

Two model simulations are described in this paper which are identical in all aspects except for their forcing. The first model (hereafter Model A) is forced only at the surface by the monthly climatological wind stresses of Hellerman and Rosenstein (1983). The second model (Model B) is forced by the same wind stresses but with the inclusion of a MOC that is forced by the northern and southern model boundary conditions. To simulate the Atlantic MOC, mass fluxes are imposed at inflow/outflow ports along the northern and southern boundaries, as shown in Table 4. Apart from these ports, all remaining parts of these boundaries are closed (and in Model A they are completely closed). At the southern boundary, a 14 Sv MOC is forced by inflow distributed in the 2nd, 3rd, and 4th model layers in the interior and western portions of the basin, and a balancing outflow in the 6th model layer at the western boundary. This distribution is intended to roughly simulate the import of thermo-

cline and intermediate waters into the South Atlantic and export of deep water by the Deep Western Boundary Current.

A similar port forcing is applied at the northern boundary, with export to the Nordic Seas in the top five layers and with compensating import (into the abyssal layer) of deep water which forms to the north of the model domain. The latter also includes the increase in the amount of NADW which occurs via entrainment by the overflow as it spills southward from the sills (Mauritzen, 1993; Schmitz, 1996). The strength of the imposed overturning cell at 65°N is 10 Sv, 4 Sv smaller than the 14 Sv cell imposed at the southern boundary. The additional 4 Sv entering the model domain via the upper ports in the southern boundary flows northward and is transferred into the deep layer in the northern part of the basin. This downwelling replaces the water lost by the bottom layer during the entrainment process which, as previously explained, maintains non-zero thickness in the upper five layers in the regions where the density surfaces would otherwise outcrop. At the same time it simulates the portion of NADW formation that occurs in the Labrador Sea (Schmitz and McCartney, 1993). This compensating global exchange from the upper layers to the abyssal layer occurs in the Labrador Sea region of the model by way of a weighting function based on the Levitus (1982) oxygen saturation data. A detailed description of this oxygen-based diapycnal mixing scheme is provided by Shriver and Hurlburt (1997). The result is a MOC in which, consistent with observations (Schmitz and Richardson, 1991; Mauritzen, 1993; Schmitz and McCartney, 1993; Schmitz, 1996), there is net northward transport above the abyssal layer, some sinking from the upper layers to the abyssal layer in the northern North Atlantic, and net southward flow in the abyssal layer.

The model bottom topography is based on ETOPO5 (NOAA, 1986) with modifications in the Caribbean region by Youtsey (1993) and Hurlburt and Townsend (1994) to correct for deficiencies in ETOPO5. Particular attention was paid to proper model representation of the sill depths and geometry of the Antilles and Bahamas passages. A notable deficiency in ETOPO5 was the presence of a wide, deep passage between the islands of Grenada and St. Vincent, which in reality is almost totally blocked by a broad shallow platform containing the Grenadines (Youtsey, 1993).

Both model simulations were begun from rest and integrated for 80 years. The last 10 years of the model results are analyzed here, after each of the models had reached statistical equilibrium. All of the mean transports, seasonal cycles, and statistics from the models are based on this final 10-year period. Analysis is confined to the top five layers of the model, which contain the wind-driven flow of the subtropical gyre and the upper ocean MOC return flow.

The analysis given here is focused on the western subtropical region of the model domain between 5°N and 30°N and west of 40°W, including the Caribbean Sea and Gulf of Mexico. A more complete discussion of the general circulation in the NRL Atlantic Basin model is given in Fratantoni et al. (2000) using a similar set of experiments, with particular focus on the equatorial Atlantic region. It is shown there that the model forced with both winds and MOC is able to reproduce a number of important features of the equatorial circulation, including the mean transports and seasonal cycles of the North Brazil Current and North Equatorial Countercurrent, the dominant time scales and general energy levels of the mesoscale eddy field, and the shedding of rings from the North Brazil Current. A weakness of the model is its unrealistic Gulf Stream separation, which does not occur near Cape Hatteras as it should but rather farther north in the model (not shown). This is due to the 1/4° resolution of this version of the model which is too coarse to achieve a realistic Gulf Stream path (Townsend et al., 2000; Hurlburt and Hogan, 2000). However, it is sufficient to obtain realistic results in other regions, including the equatorial Atlantic and the Caribbean Sea region. At a resolution of 1/4°, all of the major passages between the Atlantic and Caribbean are represented in the model, even though the narrowest ones may contain as few as one or two model gridpoints. Thus the detailed flow structure in these passages is not well resolved by the model.

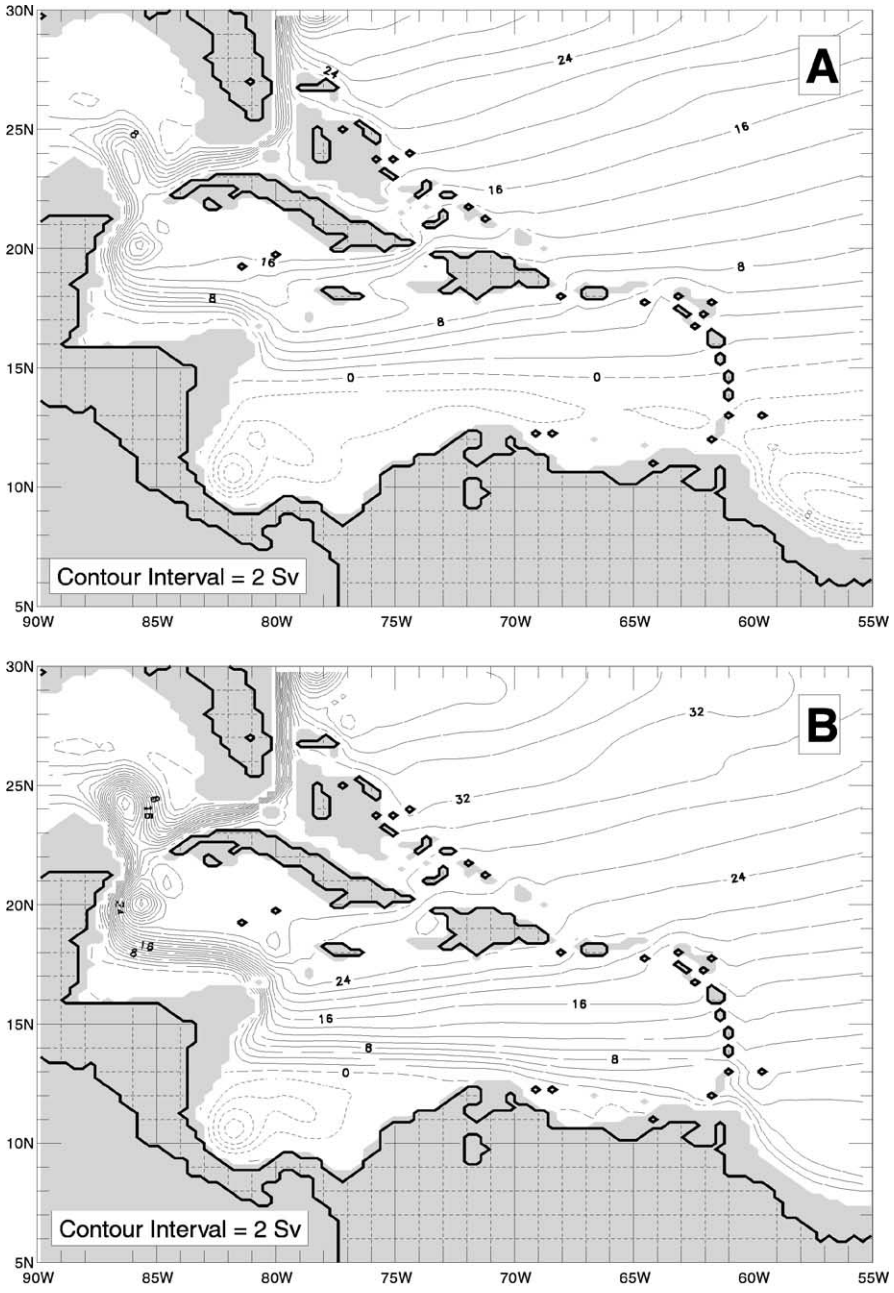

Fig. 3. Ten-year average streamfunction for the upper five model layers (< 1000 m), for (a) Model A (wind-forced only) and (b) Model B (combined wind/MOC-forced).

However, preliminary comparisons with other model simulations at higher resolution (up to 1/32°) suggest that the passage transports themselves are not highly sensitive to changes in resolution, provided that all of the major passages are open in the model.

4. Model results

4.1. Annual mean inflow to the Caribbean

The mean flow structure in the Caribbean region of the two model experiments is illustrated in Fig. 3 by 10-year mean transport streamfunctions for the sum of the top five layers. Vertical mass exchange between the 5th and 6th model layers is negligible in both models, and therefore a closely approximate streamfunction can be computed for the top five layers as a whole. This is not true in general for individual layers because of regionally varying vertical mass exchanges, even though the total mass of each layer is conserved over the entire model domain (Wallcraft, 1991). Most of the discussion will therefore center on the total transport of the top five layers.

We begin by discussing the principal features of the wind-driven model and its relation to the Sverdrup circulation. Changes in the circulation and transport distribution in the Caribbean region with the addition of a MOC are then discussed, and the two models are compared with observations.

4.1.1. Model A: wind forced

In the interior region, away from the western boundary, the annual mean circulation in the wind-forced model (Fig. 3a) should be largely reflective of the climatological mean Sverdrup circulation. As a starting point we therefore consider what the implications are for inflow to the Caribbean assuming the circulation would be in non-topographic Sverdrup equilibrium. The annual mean Sverdrup streamfunction calculated from the same (Hellerman and Rosenstein) winds used to drive the model is shown in Fig. 4, which contains the following main characteristics. The total Sverdrup transport of the subtropical gyre is slightly more than 30 Sv, of which approximately 25 Sv impinges on the Bahamas/Antilles island arc south of 27°N (the latitude of the northern Bahamas). The southern limit of the subtropical gyre intersects the Lesser Antilles at about 15°N, south of which there is approximately 5 Sv of additional flow impinging on the Antilles associated with the cyclonic tropical gyre. If one applies conventional Sverdrup theory (i.e., neglecting the island chain topography and closing the Sverdrup streamlines with the required western boundary currents), the transport of the Florida Current exiting through the Straits of Florida at 27°N would be just equal to the subtropical gyre transport south of that latitude, or approximately 25 Sv. Similarly, the flow entering the Caribbean south of 15°N in the tropical gyre would have to turn southward in the western Caribbean to form an *eastward* directed boundary current along the southern margin of the basin, ultimately flowing back out of the Caribbean and southward to close the tropical gyre. The general inflow distribution to the Caribbean predicted by Sverdrup theory would then consist of a relatively uniform inflow along the Island arc, totaling approximately 30 Sv, and a concentrated outflow of approximately 5 Sv in the far southern Caribbean.

The circulation of Model A has many similarities to this description but some important differences. The meridional distribution of the interior transport impinging on the island arc is quite similar to the Sverdrup distribution, as is the location near 15°N of the zero contour marking the tropical–subtropical gyre boundary. Deflection of the flow by the island chain is evident in several locations, for example, near 18°N where the flow is diverted northward around the northernmost islands in the Lesser Antilles, and along the Bahamas where flow is steered to the north as it approaches the boundary and a portion escapes to the east of the Bahamas to join the Gulf Stream farther north. A major difference between the model and Sverdrup results is the blocking of the tropical gyre inflow to the southern Caribbean by the Windward Islands. Most of the tropical gyre flow carried westward by the North Equatorial Current in the model is turned southward outside the island arc, leading to two separate cyclonic gyres inside and outside the Caribbean that are only weakly connected by recirculating flow through the passages. The inflow distribution occurring in this model is remarkably similar to that found in a simpler linear, reduced-gravity model driven by the same winds (Townsend et al., 2000). Nonlinear effects are evident in the model in the form of small inertial recirculation gyres in the

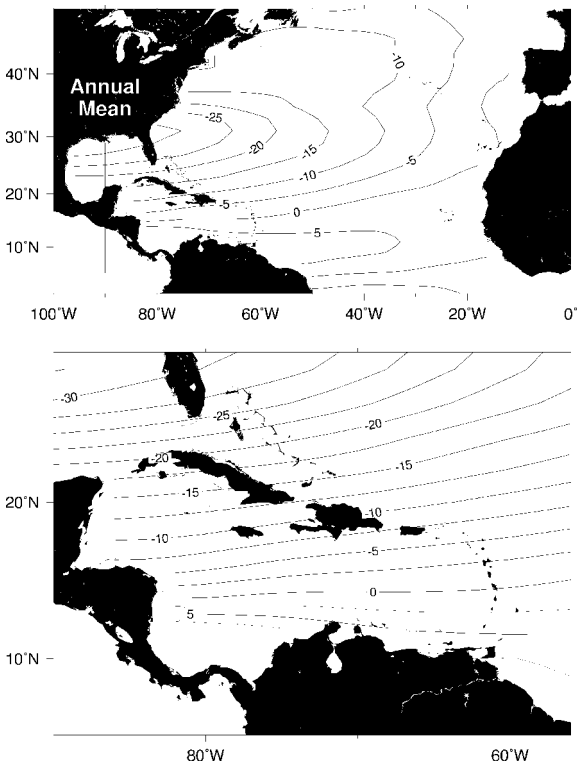

Fig. 4. The annual mean Sverdrup streamfunction derived from Hellerman and Rosenstein (1983) winds. These are the same winds used to drive the model simulations. The region surrounding the Carribean Sea is magnified in the bottom panel for closer comparison with Fig. 3.

western Caribbean, off Panama and just south of Yucatan Channel.

The mean transports for this model through each entry and exit passage bordering the Caribbean Sea are shown in Fig. 5a. The transport of the Florida Current in this model is only 21.3 Sv, roughly 10 Sv less than the actual Florida Current transport. Combined with the northward transport off Abaco Island in the northern Bahamas (3.3 Sv), the total northward flow along the western boundary is 24.6 Sv, just balancing the ~25 Sv of Sverdrup flow incident on the western boundary south of 27°N. The largest inflow contribution to the Caribbean occurs through Windward Passage (7.4 Sv), with other passages contributing between 1 and 3 Sv of inflow. Transport through the southernmost (Grenada) passage is out of the Caribbean at 2.1 Sv, balancing the 2 Sv of net inflow coming through the St. Vincent and St. Lucia passages just to its north. This is consistent with the above expectations from Sverdrup theory, even though the total recirculation of water through these passages in the model is much smaller than the Sverdrup requirement. The reasons for this may have to do with the fact that the return current required by Sverdrup theory exiting the southern Caribbean cannot, in reality, be infinitesimally thin, in which case it will directly oppose the Sverdrup inflow and could lead to a significant reduction in the total water exchange. Partial blocking of the inflow by the narrow channels and the shallow Grenadines platform could also contribute to this limited exchange. In either case, an important result of both the model and the Sverdrup prediction is that the net wind-forced inflow from the Atlantic to the Caribbean south of 15°N (near the latitude of Martinique) is approximately zero. Thus, in the model as well as the Sverdrup prediction, the wind-driven inflow feeding the Florida Current is derived entirely from the subtropical gyre inflow which enters the Caribbean north of the climatological tropical/subtropical gyre boundary at ~15°N.

4.1.2. *Model B: wind and MOC forced*

The total inflow to the Caribbean and its distribution among the passages changes considerably with the addition of a 14 Sv MOC (Figs. 3b and 5b). The transport of the Florida Current at 27°N rises by 11 to 32.3 Sv, nearly in agreement with the established value of 31.5 Sv (Lee et al., 1996). The distribution of the transport among the various passages, and the differences between the two models, are illustrated more clearly in Fig. 6. The largest changes occur in the southernmost passages, where the 2.1 Sv outflow from Grenada Passage in Model A is reversed to an inflow of 5.0 Sv (a net change of 7.1 Sv), and the inflow in St. Vincent Passage increases from 1.1 to 5.2 Sv (a net change of 4.1 Sv). The total inflow to the Caribbean through the Windward Islands passages (Grenada, St. Vincent, and St. Lucia) is now 12.3 Sv, as compared to essentially zero in the wind-driven model.

The remaining passages, with the exception of Windward Passage, show smaller changes of

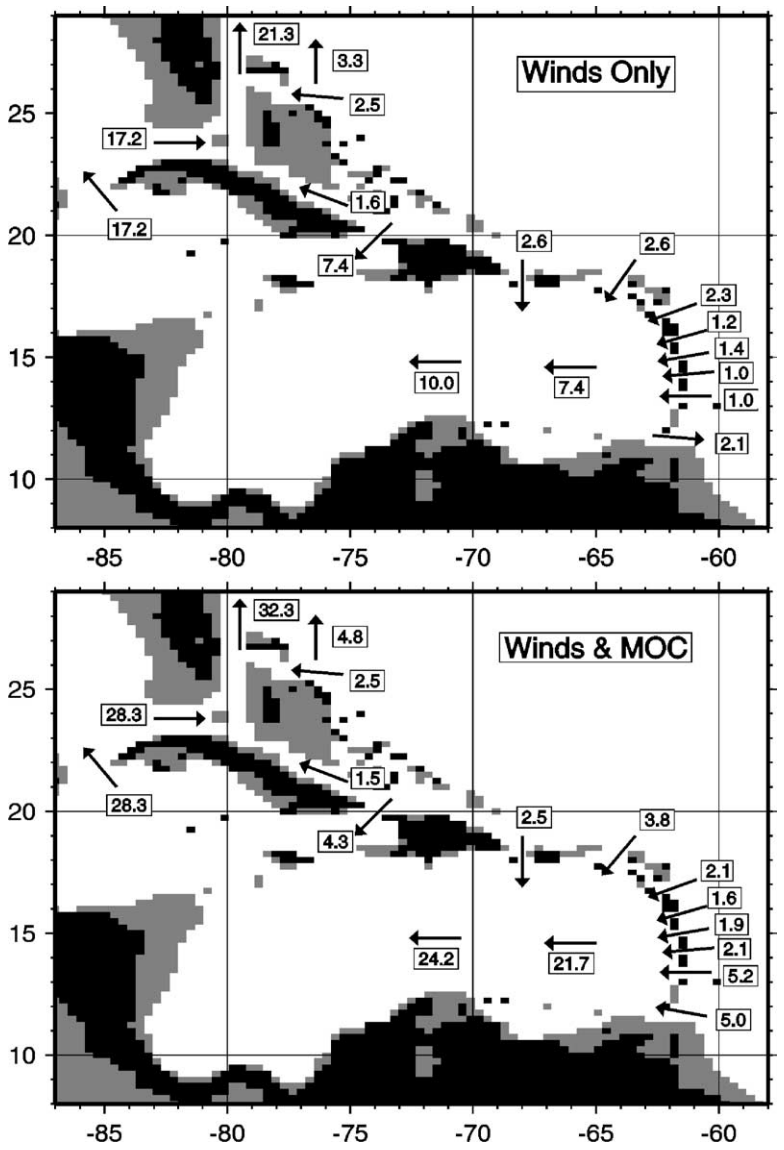

Fig. 5. Mean (10-year average) transports through all of the major Caribbean passages for both models: (a) wind-forced, and (b) combined wind/MOC-forced.

typically 1 Sv or less, with a general pattern of increased inflow through the Lesser Antilles Passages and decreased inflow through the northern (Greater Antilles) passages. The sum of all the transport differences south of Windward Passage (Grenada through Mona Passage) is 14.2 Sv, which indicates that all of the MOC-driven flow is entering the Caribbean through the Lesser Antilles Passages. The additional inflow derived from the MOC is, however, clearly concentrated in the far southern Caribbean.

One unexpected result from these models is the large decrease in inflow through Windward Passage of approximately 3 Sv with the addition of the MOC. This change appears to be due to a modification of the inflow pattern from the

subtropical gyre to the Caribbean caused by the addition of the MOC. In Model B, more of the subtropical gyre flow that impinges on the southern Bahamas is diverted northward toward Abaco rather than feeding through the small channels in the Bahamas toward Windward Passage. The northward transport off Abaco increases to 4.8 Sv in Model B, which indicates that more of the subtropical gyre flow closes off east of the Bahamas than in the wind-only experiment.

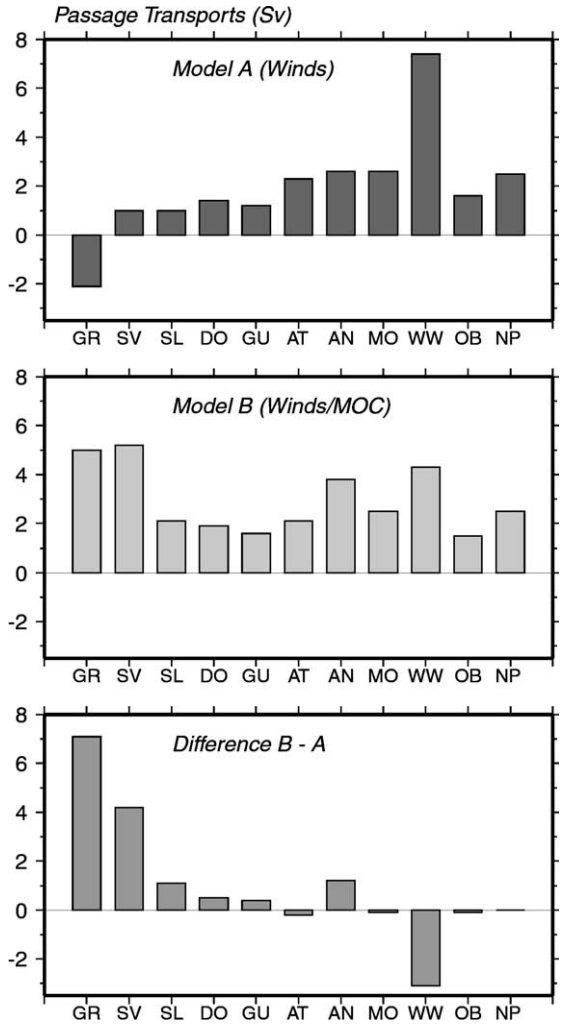

Fig. 6. Distribution of passage transports along the Antilles arc, from south (left) to north (right), for (a) the wind-forced model, and (b) the combined wind/MOC-forced model. Abbreviations for each passage are: GR (Grenada), SV (St. Vincent), SL (St. Lucia), DO (Dominica), GU (Guadeloupe), AT (Antigua), AN (Anegada), MO (Mona), WW (Windward), OB (Old Bahama), and NP (NW Providence). The difference in passage transports between the two models (b–a) is shown in panel (c). The additional inflow from the MOC is strongly concentrated in the southern Caribbean passages.

The results of these two experiments suggest the following main conclusions on the causes and distribution of the total inflow entering the Caribbean Sea in the models:

1. The wind-driven inflow to the Caribbean from the subtropical gyre occurs mainly north of 15°N, near the latitude of Martinique.
2. The 14 Sv MOC flow in Model B enters the Caribbean through the Lesser Antilles passages, and is strongly concentrated in the southernmost passages to the Caribbean.
3. The entire MOC flow continues westward through the Caribbean Sea and Yucatan Channel to exit northward through the Straits of Florida.
4. The difference of 11 Sv between the Florida Current transport in the two models, which is 3 Sv smaller than the total MOC strength, is due to a decrease of approximately 3 Sv in the subtropical gyre inflow to the Caribbean through Windward Passage, which instead turns northward outside the Caribbean to join the Gulf Stream east of the Bahamas.

4.2. The seasonal inflow cycle

Superimposed on the mean inflows discussed above, the models show both seasonal variations and large-amplitude intraseasonal variations in the passage transports. We describe first the seasonal cycle of inflow in the model, followed by a discussion of the shorter time scale fluctuations. Since the MOC forcing in the model is steady, the seasonal fluctuations in the model are forced primarily by the winds, which are the same in both models. Therefore we discuss only the seasonal cycle for Model B, which has the most realistic total forcing. The mesoscale variablility is quite different in the two models, however, and both model results are shown. Later the results are compared to observations, including the known Florida Current seasonal cycle and available time

series current records in some of the passages, and also with previously published model predictions (e.g., Anderson and Corry, 1985).

Time series of the 10-year modeled transports through a subset of the passages along the Lesser Antilles are shown in Fig. 7. The dominant feature of these transports is the large seasonal cycle in the southern passages, which decreases in amplitude toward the north. The seasonal transport cycles through the Windward Islands, Leeward Islands, and Greater Antilles passages computed from the 10-year model time series are shown in Fig. 8, along with the seasonal cycle from Yucatan Channel, which equals the sum of these transports. A comparison of the model annual cycle with observations in the Straits of Florida is shown in Fig. 9.

The Windward Islands have by far the largest seasonal cycle of the three passage groups, with a total annual range of 6 Sv (Fig. 8). The transport cycle here is highly asymmetrical, with a maximum in June and a minimum in September–October. Most of this seasonal cycle is contained in Grenada Passage. Besides the Grenada and St. Vincent Passages, none of the other individual passages exhibit a climatological seasonal range of more than 1 Sv. The Leeward Island Passages have a combined annual range of approximately 2 Sv with a maximum inflow in September and minimum in June, a cycle that is nearly out of phase with that in the Windward Islands passages. The flow through the Greater Antilles passages has an annual range of ~ 2 Sv and is semiannual in character, with maxima occurring in April and September.

The model outflow from the Caribbean through Yucatan Channel (and the Straits of Florida) is characterized by a fall minimum in October, and a broad, nearly featureless maximum from February to July. In general this cycle closely resembles the inflow cycle through the Windward Islands Passages. The main differences are (1) the fall minimum is shifted 1 month later to October–November (owing to the September inflow maximum through the Leeward Islands and Greater Antilles), and (2) the summer inflow maximum through the Windward Islands is mostly canceled by the opposing summer inflow minima through the Leeward Islands. Overall it is clear that the Yucatan Channel (and Florida Straits) transport cycle in the model derives its main characteristics from the Windward Islands transport cycle in the far southern Caribbean.

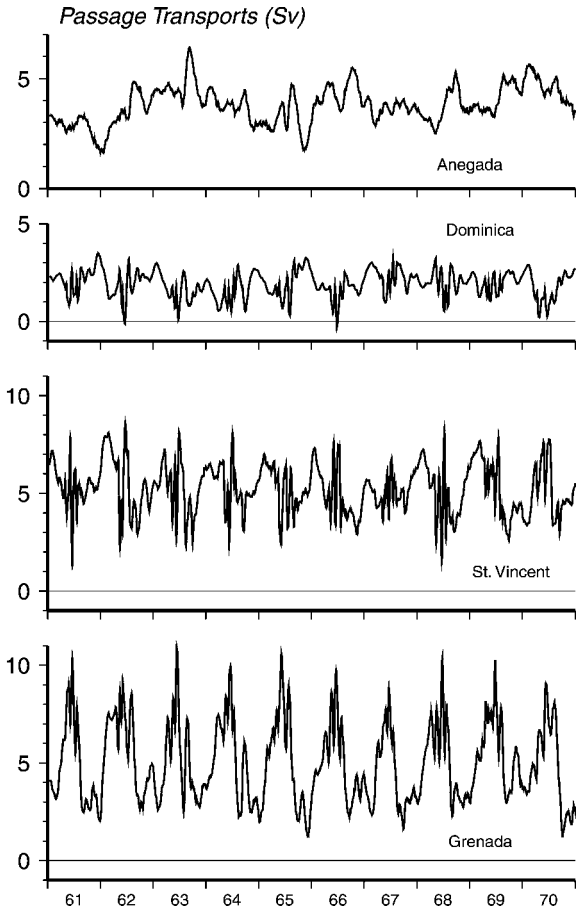

Fig. 7. Ten-year time series of passage transports for selected passages, from south (at the bottom) to north (at top) along the Lesser Antilles, from the combined wind/MOC forced model (Model B). The southern passages (e.g., Grenada and St. Vincent) are characterized by the strongest seasonal variation and also by strong intraseasonal variations on time scales of 1–2 months.

The seasonal cycle of the Florida Current produced by the model is in reasonable agreement with observations (Fig. 9). Earlier experiments with NRL Atlantic Basin model have also shown good success in predicting the Florida Current's seasonal cycle (e.g., Thompson et al., 1992). The

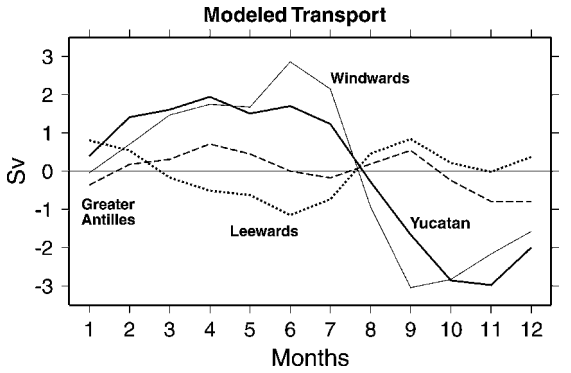

Fig. 8. Annual transport cycles for the Yucatan Current (bold line) and the main passage groups that supply it: the Windward Islands passages (thin line), the Leeward Islands passages (dashed line) and the Greater Antilles passages (dotted line).

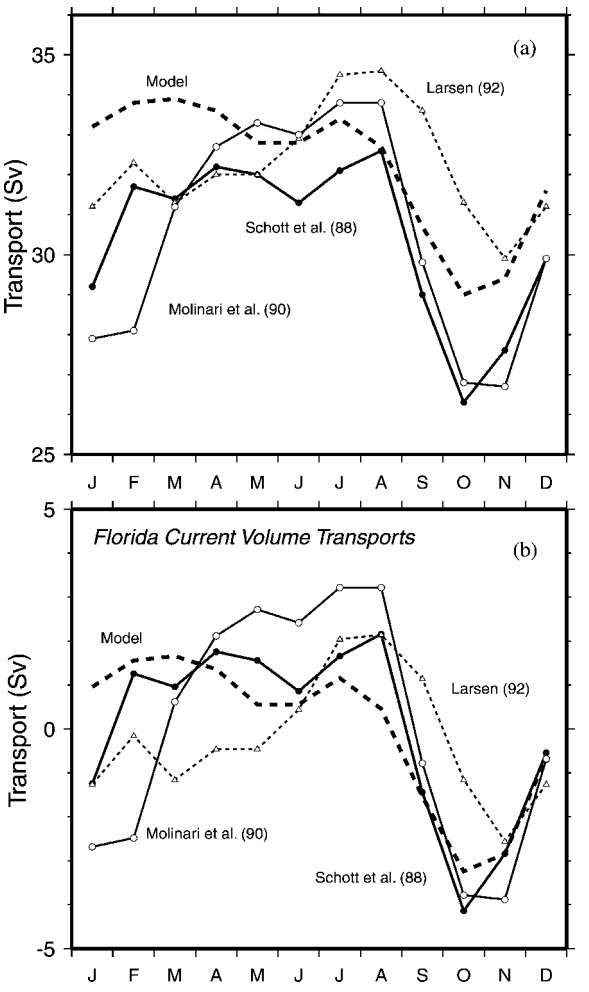

Fig. 9. The modeled annual cycle of the Florida Current at 27°N (bold dash line), compared with observed estimates of the annual cycle. The top panel shows the absolute transports; the bottom panel compares only the seasonal variation by showing the monthly variations about the annual mean transport for each curve.

mean transport of the model Florida Current (32.3 Sv) is somewhat higher than the mean values of 30.5 determined by Schott et al. (1988) and 30.6 Sv by Molinari et al. (1990) but shows an annual cycle very similar to their results, especially those of Schott et al. (1988). Leaman et al. (1987) reported a higher value for the mean transport of 31.7 Sv, and Larsen (1992) gives an even higher mean transport of 32.3 Sv based on longer term cable observations, but finds a seasonal cycle with a less-pronounced fall minimum than the earlier studies. The only clearly disputable feature of the model-predicted transport is the fact that its absolute maximum occurs in spring (March) rather than during summer as seen in all of the observational results. Apart from this feature the model can be said to produce an adequate representation of the Florida Current annual cycle, and therefore has merit for studying the related transport cycles in the broader Caribbean region.

To better understand the cause of the seasonal cycle in the model and the linkages of the transport variations throughout the basin, we show in Fig. 10 the upper ocean (layers 1–5) transport streamfunction for the months of April and October, which are near the maximum and minimum transports of the Florida Current in the model. The overall pattern of inflow is similar for these months except in the far southern Caribbean where the streamlines entering the basin are more strongly concentrated in the south during April, especially on the Atlantic side. The inflow to the southern Caribbean at this time appears to result from a direct northward transport of waters from near the equator in an intensified western boundary current (a "Guyana" Current) that enters the Caribbean through the Windward Islands passages. Conversely, during October, a cyclonic circulation cell (or trough) develops just southeast of the Lesser Antilles along 10°N that blocks the direct inflow of South Atlantic water to

the Caribbean along the western boundary. The development of this trough coincides with the northward migration of the Intertropical Convergence Zone (ITCZ) from near the equator in late winter to near 10°N in fall, and the associated intensification of positive (cyclonic) wind stress curl at these latitudes across the western Atlantic. The northward flow of South Atlantic waters along the western boundary at this time is diverted offshore in the North Brazil Current Retroflection (just visible in the lower part of the figure) to feed the eastward flowing North Equatorial Countercurrent. Since the MOC-driven flow in the model is steady, this water must (and does) eventually flow northward in the interior, and later enters the Caribbean via the westward-flowing North

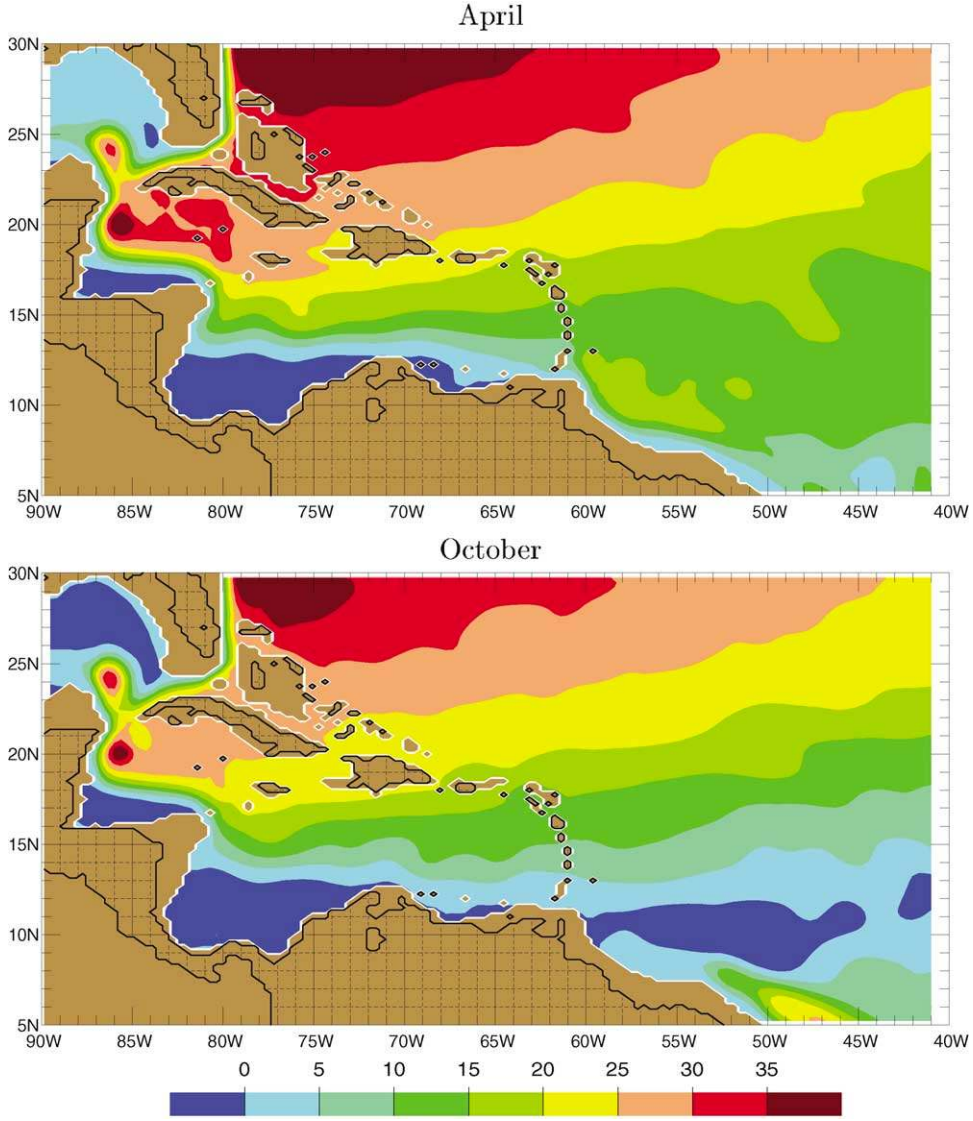

Fig. 10. Transport streamfunction of the top 5 model layers (<1000 m) for the months of April and October (10-year climatology). Differences in the two seasons are most apparent in the tropical Atlantic and southern Caribbean.

Equatorial Current. Thus the changes in the inflow structure, even though driven entirely by changes in the seasonal winds, involve significant changes in the pathways of the thermohaline (MOC-driven) flow in the model and its entry to the Caribbean. Similar results were obtained by Fratantoni et al. (2000) and are discussed in greater detail there for the broader tropical Atlantic region (see also Mayer and Weisberg, 1993; Philander and Pacanowski, 1986). The mean streamline patterns shown in Fig. 3b reflect this seasonal partitioning, where both a western boundary and interior pathway can be seen in the annual mean streamfunction field.

Other, more subtle, differences occur in the seasonal streamline patterns that are better illustrated in Fig. 11, which shows the streamfunction anomalies relative to the annual mean every 2 months through the year. As before, the dominant feature is the large scale cyclonic circulation anomaly that develops along about 10°N in fall (Aug.–Dec.), which is replaced by an opposite anticyclonic anomaly in the same region during winter and spring (Feb–June). This is again consistent with the changes in wind stress curl over this region associated with the meridional migration of the ITCZ. During summer (June) this anticyclonic circulation anomaly (shown by red shades in Fig. 11) can be seen to spread westward into the Caribbean reaching all the way to Central America. It should be noted that since we are considering just the top five layers of the model, down to about 1000 m, the changes shown in Fig. 11 represent mainly a baroclinic response of the circulation to the seasonal wind forcing. This summer anticyclonic anomaly leads to intensified inflow through the Windward Islands passages (mainly Grenada Passage), and a corresponding outflow anomaly (or reduced inflow) through the Greater Antilles and northern Leeward Islands passages. It is this feature that explains the summer inflow maximum through the Windward Islands passages in the southern Caribbean.

By August, this feature has mostly decayed and is replaced by a growing cyclonic anomaly (shown by the blue shades in Fig. 11) that spreads westward into the Caribbean. This produces a relative outflow anomaly (or inflow minimum) through the southern passages in October. However, unlike the summer anticyclonic anomaly, which remains mostly confined to the tropics and central Caribbean Sea, the fall cyclonic anomaly encompasses a broad region including the southern part of the subtropical gyre, while still being most intense east of the Antilles. Thus, during October, one can trace the negative (outflow) transport anomaly in Grenada Passage all the way through the Caribbean Sea to the Straits of Florida, where it corresponds to the minimum annual transport through both channels. This suggests a strong dynamical link between the southern Caribbean passages and the Florida Current with regard to seasonal transport fluctuations, especially for the fall transport minimum in the Florida Current. In the summer there is no corresponding transport maximum in the model Florida Current, because the inflow maximum through the Windward Islands passages is largely canceled by the broad outflow anomaly through the northern passages. That is, the anticyclonic cell in summer mostly closes off on itself within the Caribbean Sea, and does not extend its influence to Straits of Florida. Other interesting features in the model include the seasonal spin-up and spin-down of the cyclonic gyre in the southwestern Caribbean (the "Panama–Colombia Gyre"), and a similar seasonal spin-up and spin-down pattern that occurs in the far western Cayman basin between 15 and 20°N. The model also indicates a seasonal modulation in the strength of the Caribbean Current, of amplitude ± 4 Sv, with maximum in summer and minimum in fall.

4.3. Intraseasonal variability

The model exhibits a vigorous intraseasonal variability in the Caribbean Sea with a dominant time scale of 1–3 months. This variability is present

Fig. 11. Maps of streamfunction anomaly from the annual mean, for the months of (a) February, (b) April, (c) June, (d) August, (e) October, and (f) December. The contour interval is 1 Sv. The monthly anomalies are derived from a 10-year model climatology. Red and yellow shades indicate a positive (or anticyclonic) anomaly; blue and purple shades a negative (cyclonic) anomaly.

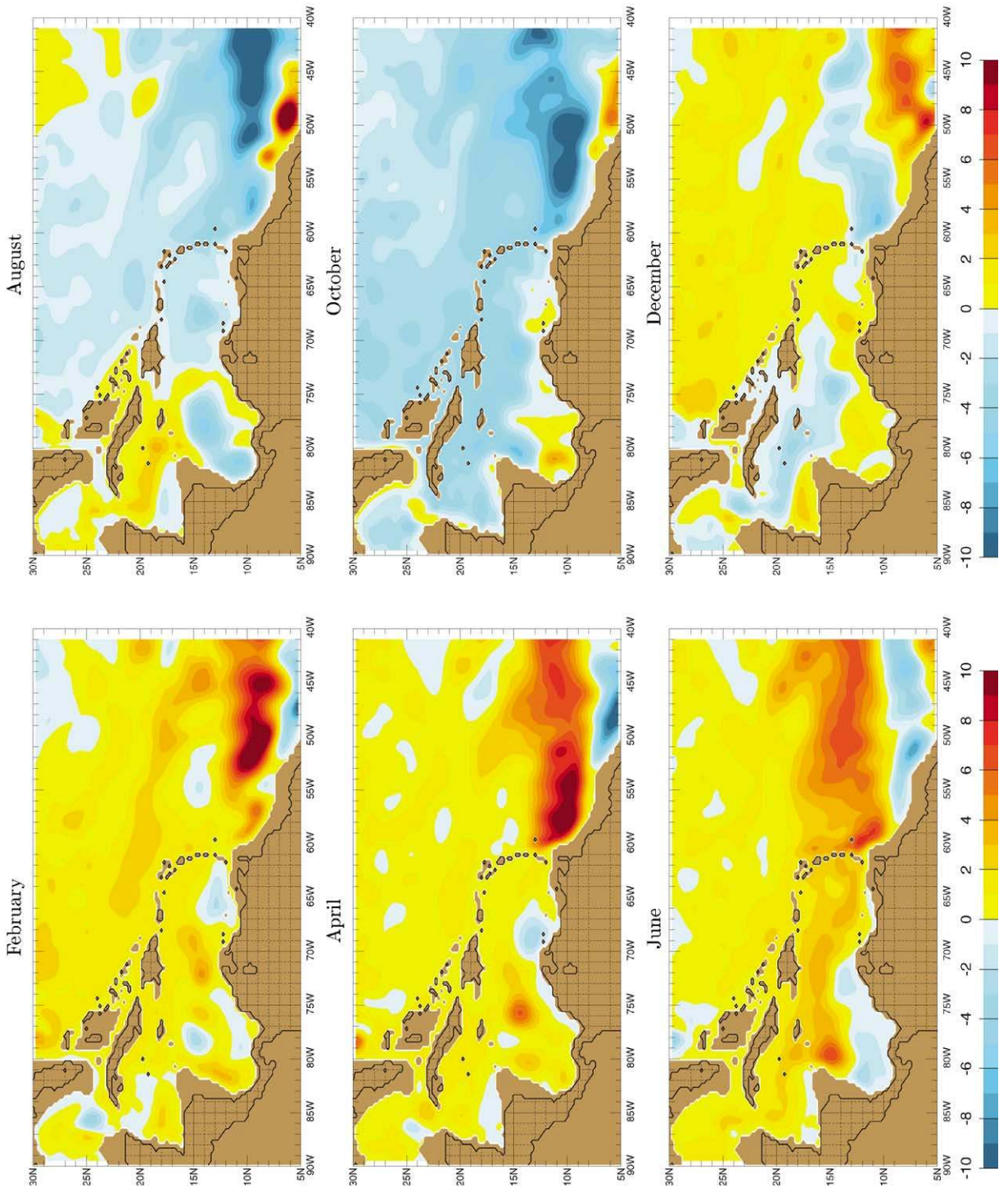
February
April
June
August
October
December
30N
25N
20N
15N
10N
5N
90W
85W
80W
75W
70W
65W
60W
55W
50W
45W
40W
-10
-8
-6
-4
-2
0
2
4
6
8
10

in both Models A and B, but it is more energetic in Model B that includes the MOC forcing (Fig. 12). The eddy kinetic energy (EKE) distributions in the model have a maximum in the western tropical Atlantic region and a secondary maximum in the Gulf of Mexico associated with the Loop Current. With the addition of the 14 Sv MOC, the EKE maximum in the western tropical Atlantic extends northward to form a pronounced tongue of elevated EKE along the seaward edge of the Lesser Antilles. In addition, the EKE levels throughout the Caribbean increase substantially and a band of high EKE develops along the axis of the Caribbean Current in the central Caribbean Sea.

The cause of the extended EKE tongue along the tropical Atlantic western boundary and Lesser Antilles in Model B can be shown clearly to be due to the shedding of eddies or rings from the North Brazil Current Retroflection. The behavior of these models is closely analogous to the model simulations studied by Fratantoni et al. (1995), where it is shown that the shedding of rings from the NBC retroflection is highly dependent on the forcing used to drive the models. In models forced only with winds, ring shedding does not occur on a regular basis and only one such feature is typically generated in each model year, usually around the time when the NECC breaks down in late winter. However, in the models that include MOC forcing, rings are shed continuously. In Model B, an average of 5–6 NBC rings are generated each year, which is in good agreement with the latest observations (Goni and Johns, 2000).

Once formed, the rings propagate northwestward along the continental margin, where they reach the Lesser Antilles in about 3 months. As the rings interact with the island chain they cause significant perturbations of the inflow through the southern passages (Fig. 7), whose amplitudes decay quickly northward along the Antilles. As an example, we show in Fig. 13 the spectrum of transport fluctuations through Grenada Passage from the two model simulations, where it is apparent that the mesoscale band is much more energetic in the simulation with the combined wind/MOC forcing. The most prominent energy peaks occur at periodicities of about 80 and 120 days, but the entire spectrum down to about 30 days is filled in with energy that is not present in the wind-only experiment. The transport fluctuations caused by the rings are comparable to the mean transports and to the amplitudes of the seasonal cycles in the southern passages. Most of the model rings move northward just outside the Lesser Antilles to as far as Anegada before completely breaking up. However, in the process they shed some of their anticyclonic vorticity anomaly through the passages, which seems to promote the development of finite amplitude instabilities on the Caribbean Current. Using a similar model, Murphy et al. (1999) show that amplifying disturbances generated in the far eastern Caribbean by NBC rings can be traced over a period of months to the area of the Yucatan Channel where they can impact the shedding of Loop Eddies in the Gulf of Mexico.

5. Discussion

5.1. Comparison of model mean transports with observations

5.1.1. The Florida and Antilles Currents

The model results presented above are generally consistent with observational studies on the sources of the Florida Current (Schmitz and Richardson, 1991), and with the present understanding of the closure of the Atlantic MOC and subtropical gyre by western boundary currents east and west of the Bahamas (Schmitz et al., 1992; Lee et al., 1996; for a review, see Hogg and Johns, 1995). Schmitz and Richardson (1991) concluded that 13 Sv of the $\sim$30 Sv transport of the Florida Current off Miami was derived from MOC flow through the southern Caribbean, leaving only a 17 Sv contribution from the subtropical gyre. Schmitz et al. (1992) postulated that this 17 Sv of wind-driven flow was supplied by 10 Sv of transport through the eastern Caribbean originating from the eastern Atlantic (Stramma, 1984) and 7 Sv through Windward Passage originating from the central and western Atlantic along 24°N. This is almost exactly the distribution that occurs in the wind-driven only model (Fig. 5a), with the remaining 8 Sv of Sverdrup transport along 27°N joining

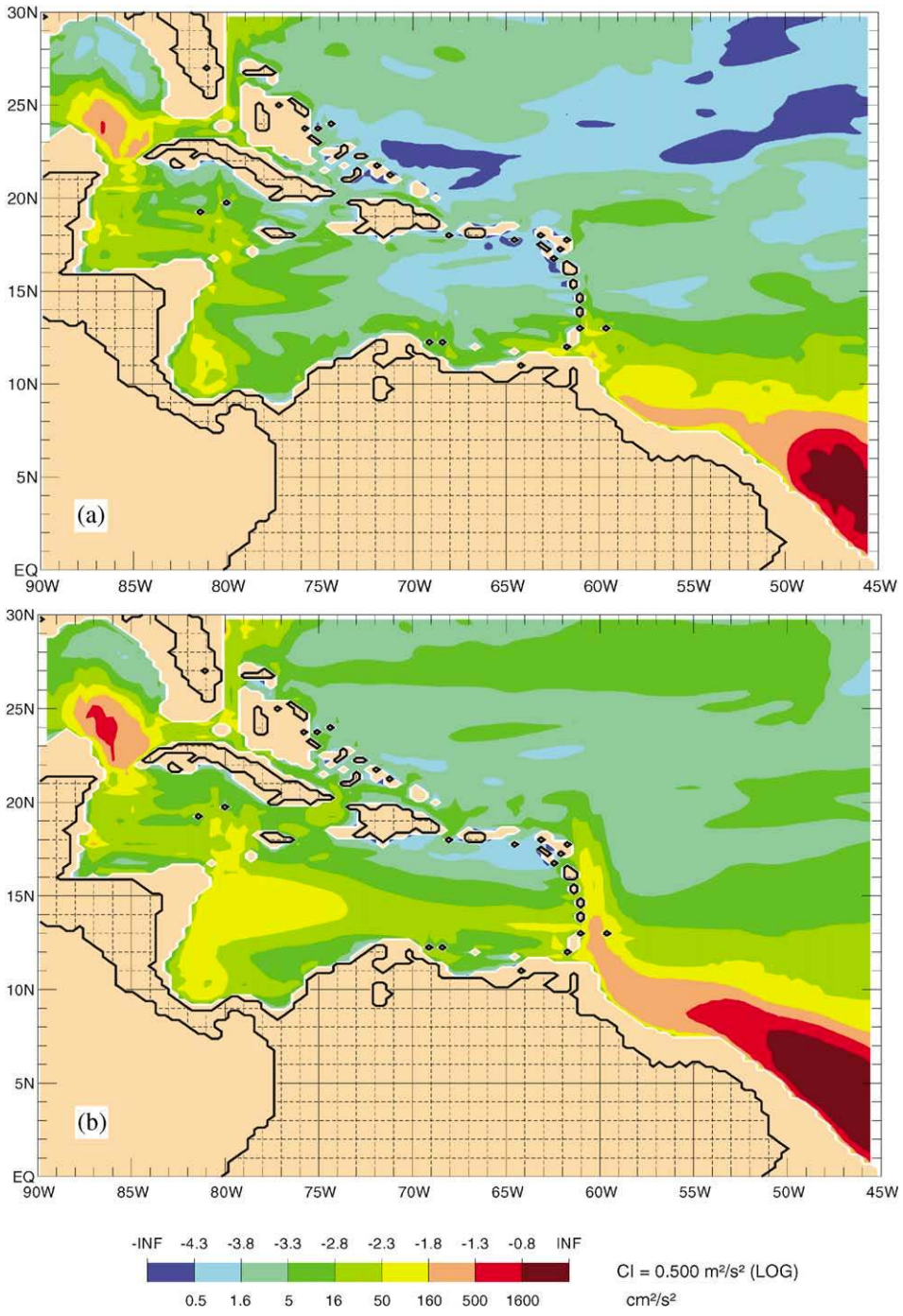

Fig. 12. Eddy kinetic energy (EKE) distributions in the broader Caribbean region from the two-model simulations: (a) wind-forced model, and (b) wind/MOC-forced model. The EKE color scale is logarithmic; corresponding values (in units of $cm^2\ s^{-2}$) are shown along the color bar.

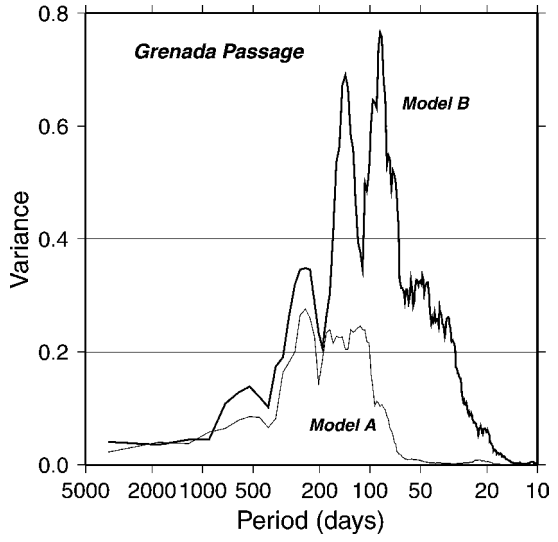

Fig. 13. Variance-conserving model transport spectra for the flow through Grenada passage in the wind-forced model (Model A—thin line) and the combined wind/MOC-forced model (Model B—bold line), after removal of the climatological seasonal cycle.

the Florida Current through the Old Bahama and Northwest Providence Channels (1.5 and 2.5 Sv, respectively), or flowing northward east of Abaco (3.3 Sv).

Lee et al. (1996) discussed the closure of the subtropical gyre along 27°N and showed that the combined transport of the Florida Current and the Antilles Current off Abaco balanced to within measurement errors the estimated Sverdrup transport at that latitude plus a 13 Sv upper ocean MOC component carried by the Florida Current. They concluded that the wind-driven component of the Florida Current was approximately 18.5 Sv (leading to a total Florida Current transport of 31.5 Sv), and that the 5.0 Sv of upper ocean transport observed off Abaco balanced the remainder of the Sverdrup transport. The total wind-driven transport carried by the Florida and Antilles currents is therefore approximately 23.5 Sv, within 2.5 Sv of the 26 Sv of southward Sverdrup transport across 27°N that Lee et al. estimated from Hellerman and Rosenstein winds. The northward transport off Abaco in the combined wind/MOC forced experiment (4.8 Sv) is, in fact, very close to the observed value of 5.0 Sv, and the Florida Current transport of 32.3 Sv is also very close to the accepted value of 31.5 Sv. The transport closure along 27°N in the model is therefore very much in accord with observations.

Obviously these comparisons are dependent on the wind climatologies used to drive the models or to compute Sverdrup transports, and the specific transport values will change with the use of different climatologies (Townsend et al., 2000). However, an important conclusion arising from these model simulations is that the use of a conventional wind stress climatology such as Hellerman and Rosenstein, with a superimposed MOC of realistic strength, leads to transport values for the Florida and Antilles Currents that are in good agreement with observations. This result differs from some other modeling studies that have suggested that the wind-stress curl and Sverdrup transport from Hellerman and Rosenstein winds are too weak and lead to an underprediction of the Florida Current transport. For example, Boning et al. (1991) found a Florida Current transport of only 23.2 Sv in a (Community Modeling Effort) (CME) simulation forced with Hellerman and Rosenstein winds, which increased to a realistic value of 29.1 Sv when forced with the wind climatology of Isemer and Hasse (1987). The Sverdrup transport along 27°N derived from the Isemer and Hasse winds is much larger, approximately 35 Sv, which, in addition to increasing the strength of the Florida Current, yields a northward transport off Abaco in the model of 12 Sv, or more than twice the observed value. The results of the present study suggest that the annual mean Sverdrup transport derived from Hellerman and Rosenstein winds is approximately correct for the subtropical North Atlantic, and that the weakness of the Florida Current in the above-mentioned CME model may be more the result of an unrealistically low MOC in that model rather than inadequacies in the wind forcing (see also: Bryan et al., 1995; Fillenbaum et al., 1997).

5.1.2. Caribbean Passage transports

The observational data base available for the eastern Caribbean passages has now reached the point where it can provide a useful constraint on

model simulations of the North Atlantic circulation (Tables 1 and 2). Fig. 14 summarizes these transport estimates from Table 2 and compares them with the results of the combined wind/MOC forced model.

The model mean transport through the Windward Islands passages for the combined wind/MOC forced experiment (Model B) is 12.3 Sv, in good agreement with the observed mean transport (10.1 ± 2.4 Sv; Table 2). The model distribution differs somewhat from the observations, suggesting a nearly equal partitioning of inflow between Grenada (5.0 Sv) and St. Vincent (5.2 Sv) passages, rather than a more important role for Grenada Passage. Of the three Windward Islands passages, only the St. Vincent Passage transport is significantly different from the observed value (2.9 ± 0.8 Sv; Table 1). However, the combined total transport of these passages is within the error bounds on the observed mean transport. We should note that the model mean transports also have some statistical "uncertainty" associated with them since they are derived from a 10-year model record with significant fluctuations, although these uncertainties are small (~ 0.2 Sv) compared to the observational uncertainties.

The net transport through the Leeward Island passages produced by the model is 9.4 Sv, again in close agreement with the observations (8.3 ± 2.3 Sv; Table 2). The modeled transports through the Dominica and Guadeloupe Passages are within the error bounds on the observed mean transport, those of the Antigua and Anegada Passages are just outside the observed error bounds. Consistent with the observed transports, the model shows a trend toward more concentrated inflow through the northern end of the Leeward Islands, even though the relative importance of Antigua and Anegada Passages is reversed between the observations and model. While discrepancies between individual passages are evident, we find again that, as for the Windward Islands Passages, the net transport through the Leeward Islands passages in the combined wind and MOC forced model is in reasonable agreement with the observed transport.

The modeled transports through Mona and Windward Passages are 2.5 and 4.3 Sv, respectively, for a total of 6.8 Sv through the Greater Antilles. The value for Mona Passage is consistent with observations, but the Windward Passage value is smaller than suggested by observations. Interestingly, the total transport through Yucatan Channel in the model is the same (~ 28 Sv) as found in observations, but is achieved by a smaller model transport of 4.3 Sv through Windward Passage (instead of ~ 7 Sv suggested by observations) and a larger net contribution of 21.7 Sv through the Lesser Antilles (instead of 18.4 Sv from observations). Given the uncertainties in the observed mean transports through the Lesser Antilles, the total inflow through the Lesser Antilles could easily be greater than the above 18.4 Sv value by 3 Sv, and therefore the Windward Passage transport value inferred from this residual calculation could be in the same range as the model value of 4.3 Sv. Also, from the available observations it appears that the Windward Passage could have a mean transport anywhere in the range of 3–9 Sv. We conclude that the model value of 4.3 Sv cannot be ruled out as a possible correct value for the mean transport through Windward Passage, although a value closer to 7 Sv appears more likely.

The results from both the model and observations indicate that the overall distribution of the Atlantic inflow to the Caribbean is nearly equally divided between the three main passage groups discussed here. The modeled and observed values for these passages are, respectively, 12.3 and 10.1 Sv for the Windward Islands passages, 9.4 and 8.3 Sv for the Leeward Islands passages, and 6.8 and ~ 10 Sv for the Greater Antilles passages. This nearly even distribution is quite different from the highly concentrated inflow through the northern Lesser Antilles proposed by Model (1950), or the concentrated inflow through the Windward Islands passages suggested by Stalcup and Metcalf (1972) and SR91. The model simulations show that this inflow distribution is governed by the combined wind and thermohaline forcing such that the Leeward Islands and Greater Antilles passages receive primarily the subtropical gyre inflow, in nearly equal amounts, while the Windward Islands passages are dominated by thermohaline inflow from the South Atlantic.

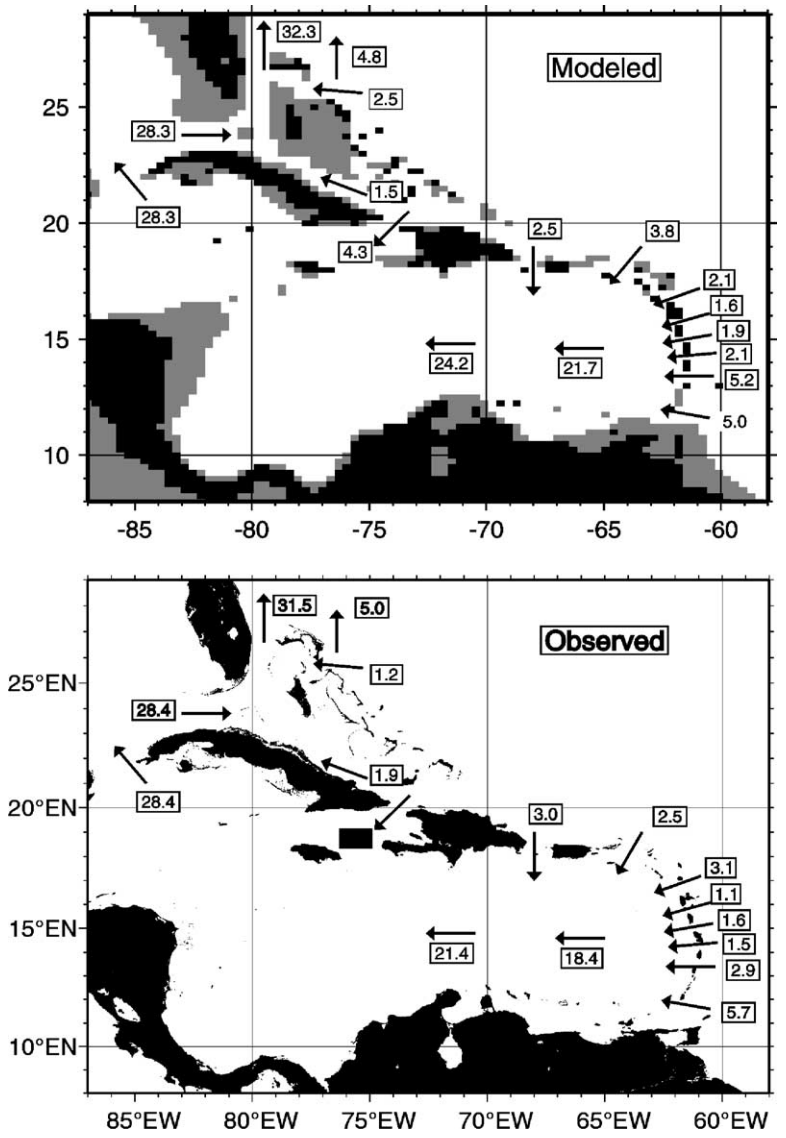

Fig. 14. Comparison of Caribbean passage transports from the combined wind/MOC-forced model simulation with observed passage transports, as summarized in Table 2.

5.2. The annual cycle

It was shown in Section 3 that the Florida Current annual cycle produced by the model was in reasonable agreement with observations. Unfortunately, there is insufficient data in any of the other passages to the Caribbean to determine the respective annual cycles for comparison with the model. The available data do, however, allow an estimate of the total range of variability in most of the passages which can be compared with the model results (Fig. 15). The overall range of variability of the passage transports predicted by the model is in good agreement with observations, with generally larger variability occurring in the southern passages. Windward Passage also shows a large transport variation in the model, which, if real, could help explain the large uncertainty in the

mean transport there from the limited observations.

The only other model study to describe the annual transport cycles in the Caribbean Passages and their relationship to the Florida Current annual cycle is that of Anderson and Corry (1985—hereafter AC85). Theirs was a two-layer model with much coarser horizontal resolution (1°) and coarser representation of topography and islands. The same seasonal wind climatology (Hellerman and Rosenstein, 1983) was used to drive the model. Only four main passages were represented in the AC85 model: the Windward Passage, Anegada Passage, and two broad channels through the Lesser Antilles. Mona Passage was blocked off in their model, and presumably the flow that would enter there is split in some way between Windward and Anegada Passages. Despite its simpler configuration this model provides an interesting comparison with the present model (Fig. 16). For a consistent comparison, the model seasonal cycles are grouped into a set of "Northern Passages" (consisting of Windward and Anegada Passages in the AC85 model, and Windward, Mona, and Anegada Passages in our model), and "Southern Passages" (which correspond to the two southern channels in the AC85 model and the sum of the Windward and Leeward Islands passages, less Anegada, in our model). The model comparison for the Yucatan Channel is also shown in Fig. 16, which is the sum of the above signals, and is nearly identical to that of the Florida Current in both models.

The seasonal cycle in the Yucatan Channel is remarkably similar for both models, with nearly the same amplitude (± 2 Sv) and phase (Fig. 16a). However, as can be seen in the lower panels of Fig. 16, this relatively small transport cycle is achieved in the AC85 model by considerably larger annual variation in the northern and southern passage groups individually than occurs in the present model. The transports vary over a range of ± 10–12 Sv annually, or three times the size of the Yucatan signal, and are nearly out of phase with each other leading to a large degree of cancellation. The phase of these signals is in general agreement with that shown by the present model but of larger amplitude. The reasons for these differences probably have to do with the smoother topography and fewer islands used in the AC85 model, resulting in deeper and wider passages, and also perhaps the very thin upper layer (100 m) used in that model. Both of these effects should tend to make the Antilles Island arc more permeable to transport fluctuations originating outside the island arc in the western Atlantic. A consistent result from both models, however, is that the transport signals in the passages around the basin are broadly connected on the seasonal time scale, and that the annual cycles in the Yucatan and Florida Currents tend to closely follow those in the southern Caribbean passages.

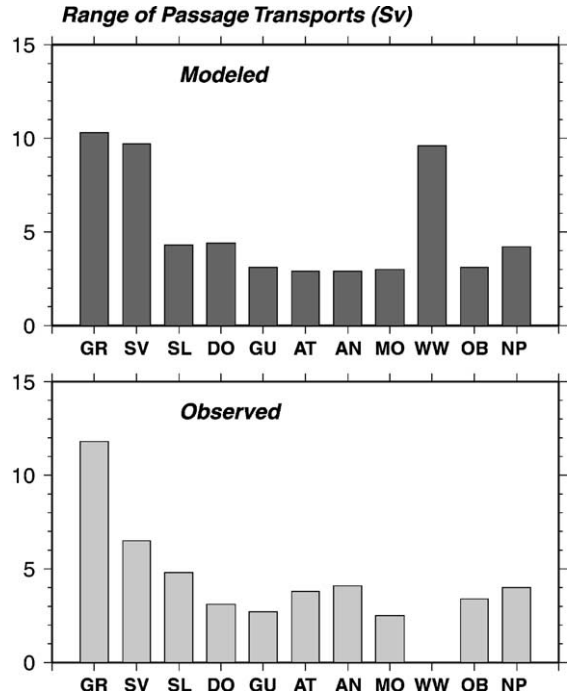

Fig. 15. Comparison of the total range of transports occurring in the various Caribbean Passages, from the model simulation (Model B) and from the available observations. The passages are arranged from south (left) to north (right) along the Antilles arc; passage abbreviations are as in Fig. 6. Insufficient data exist to determine a reliable range of observed transport in Windward Passage (WW).

Concerning the failure of the present model to reproduce the observed summer maximum of the Florida Current transport, it seems possible that this feature could result from the same type of basinwide response that occurs in the model

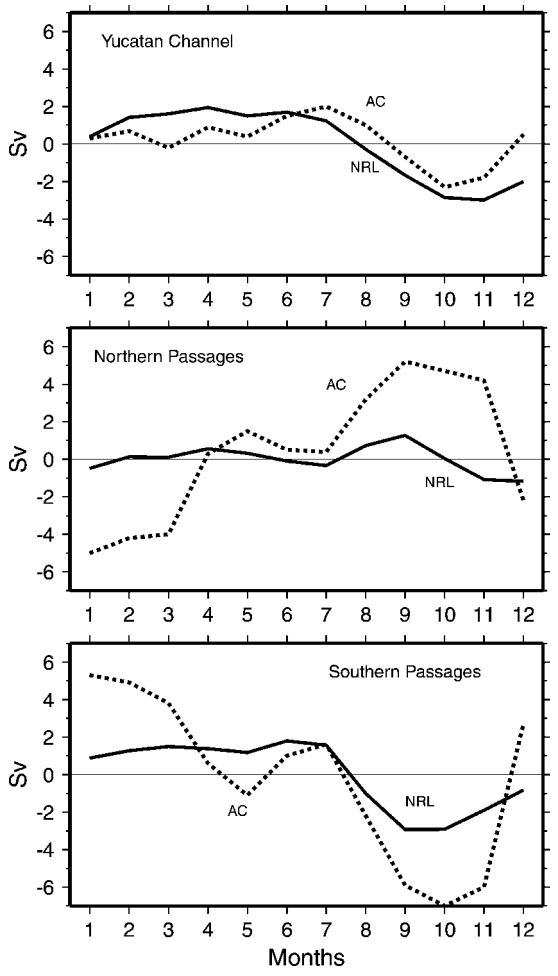

Fig. 16. Model annual transport cycles compared with those of the Anderson and Corry (1985) model, for (a) Yucatan Channel, (b) the "northern" Caribbean Passages, and (c) the "southern" Caribbean passages. See text for the definitions of "northern" and "southern" passages for the two models.

during the fall, but that this response is somehow not properly simulated in summer by the model. The low-latitude response in the summer is virtually a mirror image of the response in fall, except that it does not penetrate far enough north in the basin to involve the Straits of Florida. This could be either a model shortcoming or a problem with the climatological winds used to drive the model. In either case, the model results strongly suggest that the seasonal transport variations though the Caribbean basin, including those in the Florida Current, are coupled to tropical wind variations and associated low-latitude baroclinic responses in the Atlantic. These features propagate or advect westward into the Caribbean in the model simulation and are principally responsible for modulating the annual mean transports through the various passages. A number of other factors may contribute to the seasonal variation of the Florida Current, including purely local forcing over the Straits of Florida (Lee and Williams, 1988; Schott et al., 1988; Böning et al., 1991), wind stress curl variations over the northern Caribbean and Gulf of Mexico (Schott and Zantopp, 1985), and wind stress forcing over topography to the north of the Straits (Anderson and Corry, 1985). A detailed study of the importance of these different mechanisms would require a study of model sensitivity to various wind forcing regions, similar to that attempted by Anderson and Corry (1985) and Böning et al. (1991), which we do not attempt here. However, the obviously strong connectivity between the the Florida Current seasonal cycle and that in the southern Caribbean passages is a robust result of the model simulations.

5.3. Intraseasonal variability

The model results suggest that an energetic variability should exist in the southern Caribbean passages on times scales of 1–3 months, caused primarily by the interaction of North Brazil Current rings with the Lesser Antilles island topography. This seems like a reasonable conclusion based on new studies of NBC rings that show them to regularly impact the Lesser Antilles (Goni and Johns, 2000). However, direct evidence for these intraseasonal passage transport fluctuations is highly limited as there are only a few long term current meter records available in the Caribbean passages. Mazeika et al. (1983) obtained current meter records in the Grenada and St. Vincent passages up to 9 months in length and found fluctuations with a dominant time scale of 50–80 days, similar to the results of the model. Though irregular and not clearly associated with eddy features east of the Antilles, these fluctuations had amplitudes comparable to the magnitude of the mean flow in the passages. The observations of

Wilson and Johns (1997; Table 1), while not providing a continuous time series, show an irregular variation of the passage transports that is strongly suggestive of an energetic mesoscale component (note that for Grenada and St. Vincent passages the tidal variability is removed from their transport estimates, and also for those estimates listed in Table 1). The inability of their data to resolve a seasonal cycle in the southern passages, despite a fairly large number of repeat occupations, is a further indication of aliasing by intraseasonal variations. For example, the highest and lowest transports observed in Grenada Passage, 10.6 and 0.1 Sv, occurred in nearly the same months (May and June) of separate years (Table 1). The model simulations suggest that the total range of variation of the passage transports is increased by about a factor of two by the addition of the mesoscale variations on top of the seasonal variation. Again the available transport observations give no specific information on the time scales, but the total range of variation of the model transports is found to be in good agreement with observations (Fig. 15).

6. Summary and conclusions

The main purpose of this paper has been to rationalize the observed inflows to the Caribbean Sea with expectations based on wind-driven theory and thermohaline forcing in the Atlantic. We show that the available observations on Caribbean passage transports have now reached a point where it is possible to construct a self-consistent mass balance for the Caribbean Sea that includes the individual contributions though each of the major passages. The net inflow to the Caribbean Sea of 28 Sv is found to be spilt approximately in equal thirds between the Windward Islands passages south of Martinique ($\sim$10 Sv), the Leeward Islands passages between Martinique and the Virgin Islands ($\sim$8 Sv), and the Greater Antilles passages between Puerto Rico and Cuba ($\sim$10 Sv). The largest individual contributions occur through Grenada Passage in the south ($\sim$6 Sv) and Windward Passage in the north ($\sim$7 Sv). Based on our review of available observations, the passage that is probably most in need of further measurements is Windward Passage, which from the available direct measurements could have a mean transport anywhere in the range of 3–9 Sv. Most of the other passages have climatological mean transports that now appear to be resolved to within 1 Sv. Thus, new measurements in Windward Passage would be a vital contribution to further understanding the transport balance of the wider Caribbean.

The results of a model simulation forced by a seasonal wind climatology (Hellerman and Rosenstein, 1983) and a 14 Sv meridional overturning cell show passage transports that are in good overall agreement with the observations. The horizontal resolution ($1/4^\circ$) of the model is just sufficient to resolve all the major passages between the Atlantic and the Caribbean Sea. The results of twin model experiments, one forced with winds alone, show that the wind-driven inflow through the Windward Islands passages in the far southern Caribbean is essentially zero, and that the large transports observed in these passages are therefore attributable to the thermohaline forcing. The subtropical gyre inflow to the Caribbean Sea is about 17 Sv, and it enters mainly through the Greater Antilles and Leeward Islands passages in the northern Caribbean, consistent with expectations from Sverdrup theory. Overall, the distribution of the passage transports shown by the models is nearly what one would expect from a linear superposition of a western intensified thermohaline flow on a wind-driven Sverdrup model of the circulation. The only significant nonlinear interaction between these modes of circulation shown in the models is a diversion of subtropical gyre waters into the northward boundary currents east of the Bahamas in the combined wind/MOC forced model, as reflected in a reduction of 3 Sv in the Windward Passage inflow in that model compared to the wind-driven model, and an increase in the northward transport off Abaco. The reasons for this are not clear, but it may have to do with the steeper north–south pressure gradient across the Caribbean that is set up by the added MOC throughflow, which may act to repel waters attempting to enter the northern part of Caribbean from the subtropical gyre.

The modeled seasonal transport cycles in the Caribbean passages show a mixed annual–semi-annual character with the largest amplitude occurring in the southern (Windward Islands) passages. The inflow to the southern Caribbean is a maximum in summer and a minimum in fall, with an amplitude of about 3 Sv. Most of this variation is contained in Grenada Passage. The Florida Current and Yucatan Current annual cycles closely follow the Windward Islands passages (Grenada) transport cycle, although they have less amplitude ($\sim$2 Sv) and slightly different phase, due to modification and partial cancellation by the northern Caribbean passage inflows. However, unlike the situation with mean transports, there is still little observational data that can be used to check or validate the model results on seasonal transport cycles in the Caribbean passages. The Florida Current annual cycle in the model is in reasonable agreement with observations, showing a pronounced fall minimum, but its absolute maximum occurs in spring rather than summer. The model results suggest that the seasonal cycles of the Caribbean passage transports are broadly connected through the basin, including the Straits of Florida, and are linked to the large seasonal adjustments that occur in the low latitude Atlantic in response to the seasonal migration of the ITCZ and associated changes in the NE trade winds. Measurements of seasonal cycles in some of the key Caribbean Passages will be an important step toward further unraveling the causes of the Florida Current annual cycle and the dynamics governing the seasonal transport variations throughout the Caribbean basin. From these simulations it appears that Grenada Passage in the far southern Caribbean would be a very important location to attempt to resolve the annual cycle.

An examination of the intraseasonal (mesoscale) variability in the models shows that an energetic 1–3 month variability occurs in the southernmost passages that diminishes rapidly in strength northward along the Lesser Antilles. North Brazil Current Rings are found to be responsible for much of the passage transport variation that occurs on these time scales. This variability appears to be directly linked to the MOC forcing and is not a feature of the wind-driven model. The overall EKE throughout the Caribbean in the combined wind/MOC forced model is also much greater than in the wind-only model. This is probably a more important "nonlinear" interaction between the wind and thermohaline forcing mechanisms than the interaction between the time-mean flows—a conclusion that may be valid not only for the Caribbean region but throughout the Atlantic and global ocean. The formation of NBC Rings appears to be a specific consequence of the addition of a strong MOC on top of a wind-driven circulation (Fratantoni et al., 1995), and this eddy mechanism in turn plays an important role in meridional watermass transport within the MOC. However, in general, it can be assumed that wherever the wind and thermohaline-driven flows reinforce each other to create stronger boundary currents (e.g., the NBC, or the Gulf Stream) there is a strong likelihood of enhanced instability and eddy activity in these regions. The Caribbean Current is increased in strength by almost a factor of two by the addition of the MOC flow, and therefore this effect may contribute to the elevated EKE levels in the Central Caribbean in addition to the direct transmission of eddy energy through the Caribbean passages. The results of this study provide further evidence that a link exists between the MOC, the formation of North Brazil Current Rings, and the variability in the Caribbean passages and the downstream eddy field in the Caribbean Sea. However, as for the seasonal variations, there is as yet little direct information available on the variation of the Caribbean passage transports on these time scales that can be compared to model predictions. More time series observations in the passages and higher resolution model simulations are needed to investigate the detailed interactions between the island chain and the eddy field in the Atlantic.

Acknowledgements

Support for this research was provided in part by the National Science Foundation under grant OCE9811531 (W.E.J. and W.D.W.) and by the National Oceanic and Atmospheric Administra-

tion under cooperative agreement NA37-RJ-0200 to the Cooperative Institute of Marine and Atmospheric Studies, Univ. of Miami (W.E.J.). W.E.J. also acknowledges support from the Office of Naval Research under contract N00014-95-1-0025. D.M.F.'s participation in this research was supported by the Koczy Fellowship from the University of Miami. Support for T.L.T. was provided by the ONR-sponsored NRL projects "Global and Basin-Scale Ocean Prediction System" (under program element 62435N) and "Dynamics of Low-latitude Western Boundary Currents" (under program element 61153N). The NRL model simulations were performed on a Cray-YMP at the Naval Oceanographic Office, Stennis Space Center, Mississippi, a component of the Department of Defense High Performance Computing Initiative. We are grateful to Bill Schmitz, Terry Joyce, Claes Rooth, and two anonymous reviewers for their helpful comments on the manuscript.

References

Anderson, D.L., Corry, R.A., 1985. Seasonal transport variations in the Florida Straits: a model study. Journal of Physical Oceanography 15, 773–786.

Atkinson, L.P., Berger, T., Hamilton, P., Waddell, E., Leaman, K., Lee, T.N., 1995. Current meter observations in the Old Bahama Channel. Journal of Geophysical Research 100 (C5), 8555–8560.

Böning, C.W., Döscher, R., Budich, R.G., 1991. Seasonal transport variation in the western subtropical North Atlantic: Experiments with an eddy resolving model. Journal of Physical Oceanography 21, 1271–1289.

Brooks, I.H., 1978. Transport and velocity measurements in St. Lucia Passage of the Lesser Antilles, Eos Transactions AGU 59 (1102), 1978.

Bryan, F.O., Böning, C.W., Holland, W., 1995. On the mid-latitude circulation in a high-resolution model of the North Atlantic. Journal of Physical Oceanography 25, 289–305.

Didden, N., Schott, F., 1993. Eddies in the North Brazil Current Retroflection region observed by Geosat altimetry. Journal of Geophysical Research 98, 20, 121–20,131.

Febres-Ortega, G., Herrera, L.E., 1976. Caribbean Sea circulation and water mass transports near the Lesser Antilles. Boletin del Instituto Oceanografico de la Universidad de Oriente 15, 83–96.

Fillenbaum, E.R., Lee, T.N., Johns, W.E., Zantopp, R., 1997. Meridional heat transport variability at 26.5°N in the North Atlantic. Journal of Physical Oceanography 27, 153–174.

Fratantoni, D.M., Johns, W.E., Townsend, T.L., 1995. Rings of the North Brazil Current: their structure and behavior inferred from observations and a numerical simulation. Journal of Geophysical Research 100 (C6), 10,633–10,654.

Fratantoni, D.M., 1996. On the pathways and mechanisms of upper-ocean mass transport in the tropical Atlantic Ocean. Ph.D. Dissertation, University of Miami, 247pp.

Fratantoni, D.M., Zantopp, R.J., Johns, W.E., Miller, J.L., 1997. Updated bathymetry of the Anegada–Jungfern Passage complex and implications for Atlantic inflow to the abyssal Caribbean Sea. Journal of Marine Research 55, 847–860.

Fratantoni, D.M., Johns, W.E., Townsend, T.L., Hurlburt, H.E., 2000. Low-latitude circulation and mass transport pathways in a model of the tropical Atlantic Ocean. Journal of Physical Oceanography 30, 1944–1966.

Garzoli, S.L., Gordon, A.L., 1996. Origins and variability of the Benguela Current. Journal of Geophysical Research 101 (1), 897–906.

Goni, G., Johns, W.E., 2001. A census of North Brazil Current rings observed from T/P altimetry: 1992–1998. Geophysical Research Letters 28 (1), 1–4.

Gordon, A.L., 1986. Interocean exchange of thermocline water. Journal of Geophysical Research 91, 5037–5046.

Gordon, A.L., 1967. Circulation of the Caribbean Sea. Journal of Geophysical Research 72, 6207–6223.

Gordon, A.L., Weiss, R.F., Smethie Jr., W.M., Warner, M.J., 1992. Thermocline and intermediate water communication between the South Atlantic and Indian oceans. Journal of Geophysical Research 97 (7), 223–227,240.

Hellerman, S., Rosenstein, M., 1983. Normal monthly wind stress over the world ocean with error estimates. Journal of Physical Oceanography 13 (7), 1093–1104.

Hogg, N.G., Johns, W.E., 1995. Western Boundary Currents, U.S. National Report to IUGG 1991–1994, Reviews of Geophysics (Suppl.)33, 1311–1334.

Hurlburt, H.E., Hogan, P.J., 2000. Impact of $1/8^{\circ}$ to $1/64^{\circ}$ resolution on Gulf Stream model-data comparisons in basin-scale subtropical Atlantic Ocean models. Dyn. Atmos. Oceans 32, 283–329.

Hurlburt, H., Thompson, D., 1980. A numerical study of Loop Current intrusions and eddy shedding. Journal of Physical Oceanography 10, 1611–1651.

Hurlburt, H.E., Townsend, T.L., 1994. NRL effort in the North Atlantic. Data assimilation and model evaluation experiments—North Atlantic Basin: Preliminary Experiment Plan. Center for Ocean and Atmospheric Modeling (COAM), University of Southern Mississippi. Report TR-2/95, 30pp.

Isemer, H.J., Hasse, L., 1987. The Bunker climate atlas of the North Atlantic Ocean, Vol. 2: Air–Sea Interaction. Springer, Berlin, 256pp.

Johns, W.E., Lee, T.N., Schott, F.A., Zantopp, R.J., Evans, R.H., 1990. The North Brazil Current retroflection:

seasonal structure and eddy variability. Journal of Geophysical Research 95 (C12), 22,103–22,120.

Johns, W.E., Lee, T.N., Beardsley, R., Candela, J., Castro, B., 1998. Annual cycle and variability of the North Brazil Current. Journal of Physical Oceanography 28 (1), 103–128.

Johns, E., Wilson, W.D., Molinari, R.L., 1999. Direct observations of velocity and transport in the passages between the Intra-Amearicas Sea and the Atlantic Ocean, 1984–1996. Journal of Geophysical Research 104 (C11), 25,805–25,820.

Larsen, J.C., 1992. Transport and heat flux of the Florida Current at 27°N derived from the cross-steam voltages and profiling data: theory and observations. Philosophical Transactions of Royal Society of London 338, 169–236.

Lee, T.N., Williams, E.J., 1988. Wind forced transport fluctuations of the Florida Current. Journal of Physical Oceanography 18, 937–946.

Lee, T.N., Johns, W.E., Zantopp, R.J., Fillenbaum, E., 1996. Moored observations of volume transport and variability in western boundary currents of the subtropical North Atlantic at 26.5°N. Journal of Physical Oceanography 26, 446–466.

Leaman, K., Molinari, R., Vertes, P., 1987. Structure and variability of the Florida Current at 27°N: April 1982–July 1984. Journal of Physical Oceanography 17, 565–583.

Leaman, K.D., Vertes, P.S., Atkinson, L.P., Lee, T.N., Hamilton, P., Waddell, E., 1995. Transport, potential vorticity, and current/temperature structure across Northwest Providence and Santaren channels and the Florida Current off Cay Sal Bank. Journal of Geophysical Research 100 (C5), 8561–8569.

Leetmaa, A., Niiler, P.P., Stommel, H., 1977. Does the Sverdrup relation account for the mid-Atlantic circulation? Journal of Marine Research 35, 1–10.

Levitus, S., 1982. Climatological atlas of the world ocean. NOAA Prof. Paper 13, US Government Printing Office, Washington, DC, 173pp.

MacCready, P., Johns, W.E., Rooth, C.G., Fratantoni, D.M., Watlington, R.A., 1999. Overflow into the deep Caribbean: effects of plume variability. Journal of Geophysical Research 104, 25,913–25,935.

Mayer, D.A., Weisberg, R.H., 1993. A description of COADS surface meteorological fields and the implied Sverdrup transports for the Atlantic Ocean from 30°S to 60°N. Journal of Physical Oceanography 23 (10), 2201–2221.

Mazeika, P.A., Burns, D.A., Kinder, T.H., 1980. Mesoscale circulation east of the southern Lesser Antilles. Journal of Geophysical Research 85, 2743–2758.

Mazeika, P.A., Kinder, T.H., Burns, D.A., 1983. Measurements of subtidal flow in the lesser Antilles Passages. Journal of Geophysical Research 88 (C7), 4483–4488.

Mauritzen, C., 1993. A study of the large-scale circulation and water mass formation in the nordic seas and Arctic Ocean. Ph.D. Dissertation, Massachusetts Institute of Technology and Woods Hole Oceanographic Institution, 221pp.

Metcalf, W.G., 1976. Caribbean–Atlantic water exchange through the Anegada–Jungfern Passage. Journal of Geophysical Research 81, 6401–6409.

Metzger, E.J., Hurlburt, H.E., 1996. Coupled dynamics of the South China Sea, the Sulu Sea and the Pacific Ocean. Journal of Geophysical Research 101, 12,331–12,352.

Model, F., 1950. Pillsburys Strommessungen und der Wasserhaushalt des Amerikanischen Mittelmeeres. Deutsche Hydrographische Zeitschrift 3, 57–61.

Molinari, R., Johns, E., Festa, J.F., 1990. The annual cycle of meridional heat flux in the Atlantic Ocean at 26.5°N. Journal of Physical Oceanography 20, 476–482.

Murphy, S.J., Hurlburt, H.E., O'Brien, J.J., 1999. The connectivity of eddy variability in the Caribbean Sea, the Gulf of Mexico, and the Atlantic Ocean. Journal of Geophysical Research 104 (C1), 1431–1453.

National Oceanic and Atmospheric Administration (NOAA) 1986. ETOPO5 digital relief of the surface of the earth. Data Announcement 86-MGG-07, National Geophysical Data Center, Boulder, Colorado.

Nelepo, B.A., Stepanov, V.N., Bulatov, R.P., Donanov, M.M., 1976. Soviet investigations of the dynamics and properties of the waters of the Caribbean Sea and Gulf of Mexico. CICAR II, Symposium on Marine Research in the Caribbean and Adjacent Regions, Caracas, FAO Fisheries Report, Vol. 200, pp. 119–131.

Niiler, P.P., Richardson, W.S., 1973. Seasonal variability of the Florida Current. Journal of Marine Research 31, 144–167.

Philander, G., Pacanowski, R.C., 1986. A model of the seasonal cycle in the Tropical Atlantic Ocean. Journal of Geophysical Research 91, 14,192–14,206.

Pillsbury, J.E., 1891. The Gulf Stream—a description of the methods employed in the investigation, and the results of the research. US Coast and Geodetic Survey Report for 1890, Appendix No. 10, pp. 459–620.

Richardson, P.L., Hufford, G.E., Limeburner, R., Brown, W.S., 1994. North Brazil Current Retroflection Eddies. Journal of Geophysical Research 99 (C3), 5081–5093.

Richardson, W.S., Finlen, J.R., 1967. The transport of Northwest Providence Channel. Deep-Sea Research 14, 361–367.

Rintoul, S., 1991. South Atlantic interbasin exchange. Journal of Geophysical Research 96, 2675–2692.

Roemmich, D., 1981. Circulation of the Caribbean Sea: a well-resolved inverse problem. Journal of Geophysical Research 86, 7993–8005.

Roemmich, D., 1983. The balance of geostrophic and Ekman transports in the Tropical Atlantic Ocean. Journal of Geophysical Research 13, 1534–1539.

Schmitz, W.J., Richardson, P.L., 1991. On the sources of the Florida Current. Deep-Sea Research 38 (Suppl. 1), 379–409.

Schmitz, W.J., Thompson, J.D., Luyten, R.J., 1992. The Sverdrup circulation for the Atlantic along 24°N. Journal of Geophysical Research 97 (C5), 7251–7256.

Schmitz, W.J., McCartney, M.S., 1993. On the North Atlantic Circulation. Review of Geophysics 31 (1), 29–49.

SchmitzJr., W.J., 1996. On the World Ocean Circulation: Vol. I, some global features/North Atlantic circulation. Woods Hole Oceanographic Institution Technical Report WHOI-96-03, 141pp.

SchmitzJr., W.J., 1996. On the World Ocean Circulation, Vol. II: The Pacific and Indian Oceans/A Global Update. Woods Hole Oceanographic Institution Technical Report, WHOI-96-08, 241pp.

Schott, F., Zantopp, R., 1985. Florida Current: seasonal and interannual variability. Science 227, 308–311.

Schott, F.A., Lee, T.N., Zantopp, R., 1988. Variability of structure and transport of the Florida Current in the period range of days to seasonal. Journal of Physical Oceanography 18 (9), 1209–1230.

Schott, F.A., Fischer, J., Reppin, J., Send, U., 1993. On mean and seasonal currents and transports at the western boundary of the equatorial Atlantic. Journal of Geophysical Research 98 (C8), 14,353–14,368.

Shriver, J.F., Hurlburt, H.E., 1997. The contribution of the global thermohaline circulation to the Pacific to Indian Ocean throughflow via Indonesia. Journal of Geophysical Research 102, 5491–5511.

Stalcup, M.C., Metcalf, W.G., 1972. Current measurements in the passages of the Lesser Antilles. Journal of Geophysical Research 77, 1032–1049.

Stalcup, M.C., Metcalf, W.G., Johnson, R.G., 1975. Deep Caribbean inflow through the Anegada–Jungfern Passage. Journal of Marine Research 33, 15–35.

Stramma, L., 1984. Geostrophic transport in the warm water sphere of the eastern subtropical North Atlantic. Journal of Marine Research 42, 537–558.

Sturges, W., 1975. Mixing of renewal water flowing into the Caribbean Sea. Journal of Marine Research 33, 117–130.

Thompson, J.D., Townsend, T.L., Wallcraft, A., Schcmitz Jr., W.J., 1992. Ocean prediction and the Atlantic Basin: scientific issues and technical challenges. Oceanography 5, 36–41.

Townsend, T.L., Hurlburt, H.E., Hogan, P.J., 2000. Modeled Sverdrup flow in the North Atlantic from 11 different wind stress climatologies. Dynamics of Atmospheres and Oceans 32, 373–417.

Wallcraft, A.J., 1991. The navy layered ocean model users guide, NOARL Report 35, Naval Research Laboratory, Stennis Space Center, MS, 21pp.

Wallcraft, A.J., Moore, D.R., 1997. The NRL layered ocean model. Parallel Computing 23, 2227–2242.

Wilson, W.D., Johns, W.E., 1997. Velocity structure and transport in the Windward Islands passages. Deep-Sea Research 44 (3), 487–520.

Worthington, L.V., 1955. A new theory of Caribbean bottom water formation. Deep-Sea Research 3, 82–87.

Worthington, L.V., 1976. On the North Atlantic circulation. The Johns Hopkins Oceanographic Studies, Vol. 6, 110pp.

Wunsch, C., Grant, B., 1982. Towards the general circulation of the North Atlantic Ocean. Progress in Oceanography 11, 1–59.

Youtsey, W.J., 1993. Report detailing modifications to the 1/8 degree global bathymetry. Sverdrup Technol. Inc., Stennis Space Center, MS.